

University of Nevada, Reno

MINES
LIBRARY
Thesis
3401

**REMOVAL OF HEAVY METAL IONS
FROM ACID MINE DRAINAGE BY MODIFIED FERRITE
CO-PRECIIPITATION PROCESS**

**A Thesis Submitted in Partial Fulfillment of the
Requirements for the Degree of Master of Science in
Metallurgical Engineering**

by

Kang Yang

Manoranjan Misra, Thesis Advisor

December, 1994

UNIVERSITY LIBRARY
UNIVERSITY OF NEVADA, RENO
RENO, NV 89557

2500176

[UAI 1995]

ACKNOWLEDGMENTS

The thesis of Kang Yang is approved:

Manojan M. R.
Thesis Advisor

Ross W. Smith
Department Chair

Ruel C. Deley
Dean, Graduate School

University of Nevada

Reno

December, 1994

ACKNOWLEDGMENTS

I express my sincere gratitude to Dr. M. Misra for my admission and his constant guidance during the entire period of my study at Department of Chemical and Metallurgical Engineering, University of Nevada, Reno. I truly appreciate Dr. R. K. Mehta for his guidance during my research work. I also thank Dr. R. W. Smith and Dr. L. C. Hsu for serving in my thesis advising committee.

I would like to acknowledge Martin Marietta Corporation and Geobiotics Inc. for giving me fellowship for my study in University of Nevada, Reno. My sincere thank to my parents, my uncles and aunts for their encouragement and support throughout my study in U. S. A.

Finally, I would like to express my gratitude to my fellow students and all the people who have given me help and encouragement.

ABSTRACT

Acid mine drainage (AMD) is a large environmental problem facing mining, mineral processing and coal preparation plants. Due to long term oxidation and weathering, sulfide bearing tailings and overburdens generate sulfuric acid and the acid dissolves heavy metals. The heavy metals contaminate groundwater, rivers and streams. Recently ferrite precipitation process has been applied to treat acid mine drainage. The conventional ferrite precipitation requires air oxidation at high temperature, or long aging time or addition of magnetite powder as promoter. In this investigation, a ferrite modified precipitation process is developed by which highly magnetic ferrite can be produced at an ambient temperature. Acid mine waters from Berkeley Pit (Montana, U.S.A.) and from Noranda Tailings (Quebec, Canada) were used. The coprecipitation of heavy metals from these two acid mine waters is studied as a function of Fe/M molar ratio, oxidation time and settling rate under applied magnetic field. The investigation indicates that the modified ferrite coprecipitation can remove substantially all of the dissolved metal ions from acid mine drainage. The ferrite product obtained after precipitation is characterized by XRD, SEM, TEM and saturation magnetization. The results show that spinel ferrite precipitate can be achieved at room temperature and the saturation magnetization of ferrite product from AMD is comparable to that of some pure ferrites.

TABLE OF CONTENTS

| | |
|---|-----|
| Signature Page ----- | i |
| Acknowledgments ----- | ii |
| Abstract ----- | iii |
| Table of Contents ----- | iv |
| List of Tables ----- | vi |
| List of Figures ----- | vii |
| 1. Introduction ----- | 1 |
| 1.1. Acid Mine Drainage ----- | 1 |
| 1.1.1. The formation of acid mine drainage ----- | 1 |
| 1.1.2. Treatments of acid mine drainage ----- | 3 |
| 1.2. Ferrites and Their Applications ----- | 5 |
| 1.2.1. Crystal structure of spinel ferrite ----- | 5 |
| 1.2.2. Conventional ferrite processing and applications ----- | 13 |
| 1.2.3. Applications of by-product ferrite ----- | 14 |
| 1.3. Ferrite Precipitations ----- | 17 |
| 1.3.1. Ferrite precipitation at high temperature ----- | 17 |
| 1.3.2. Ferrite precipitation at room temperature ----- | 19 |
| 1.4. Ferrite Coprecipitation of Heavy Metals from Waste Water ----- | 21 |
| 1.4.1. General ferrite process for the treatment of waste water containing heavy metals ----- | 21 |
| 1.4.2. Modified ferrite process for the treatment of waste water containing heavy metals ----- | 23 |
| 1.5. Mechanism of Ferrite Precipitation ----- | 24 |
| 1.5.1. Mechanism of ferrite precipitation at high temperature ----- | 24 |

| | |
|---|----|
| 1.5.2. Mechanism of ferrite precipitation at room temperature ----- | 28 |
| 1.5.3. Mechanism of ferrite precipitation with ferrite promoter ----- | 32 |
| 2. Experimental ----- | 33 |
| 2.1. Materials ----- | 33 |
| 2.2. Apparatus ----- | 33 |
| 2.3. Procedures ----- | 33 |
| 2.4. Measurements of Properties ----- | 37 |
| 3. Results and Discussion ----- | 38 |
| 3.1. Synthetic Solutions of $\text{FeSO}_4 \cdot 7\text{H}_2\text{O}$ ----- | 38 |
| 3.1.1. Effect of air oxidation time on oxidation reduction potential (ORP) ----- | 39 |
| 3.1.2. Effect of air oxidation and aging time on magnetic settling ----- | 44 |
| 3.1.3. The characteristic of precipitates ----- | 55 |
| 3.2. Ferrite Coprecipitation of Noranda Tailing Water ----- | 55 |
| 3.2.1. The settling rate of precipitates from Noranda Tailing Water ----- | 61 |
| 3.2.2 The results of treatment of Noranda Tailing Water and characteristics of the precipitate ----- | 61 |
| 3.3. Ferrite Coprecipitation of Berkeley Pit Water ----- | 65 |
| 3.3.1. The settling rate of precipitates from Berkeley Pit Water ----- | 65 |
| 3.3.2. The results of treatment of Berkeley Pit Water and characteristics of the precipitate ----- | 65 |
| 3.4. Mechanism of New Modified Ferrite Coprecipitation ----- | 75 |
| 3.4.1. Reaction mechanism of initial oxidation ----- | 75 |
| 3.4.2. Reaction mechanism of air oxidation ----- | 75 |
| 3.4.3. Reaction mechanism of aging ----- | 76 |
| 4. Summary and Conclusions ----- | 78 |
| 5. References ----- | 79 |

LIST OF TABLES

| | |
|--|----|
| Table 1.1. Arrangements of Metal Ions in the Unit Cell of a Ferrite $\text{MO-Fe}_2\text{O}_3$ ----- | 12 |
| Table 1.2. Saturation Magnetization and Lattice Parameter of some Ferrites ----- | 13 |
| Table 1.3. Concentration (mg/l) of Heavy Metals in Influent and Effluent from Laboratory Wastewater ----- | 23 |
| Table 3.1. Effect of Oxidation Time on ORP, Color and Magnetic Property ----- | 38 |
| Table 3.2. Temperature and Oxidation Time to Obtain Strong Magnetic Precipitate ----- | 47 |
| Table 3.3. Concentration of Heavy Metals in Noranda Tailing Water and Treated Water ----- | 60 |
| Table 3.4. Concentration of Heavy Metals in Berkeley Pit Water and Treated Water ---- | 68 |
| Table 3.5. Comparison of Saturation Magnetization of Ferrites ----- | 71 |
| Figure 1.1. Schematic diagram of separating settling height rate of precipitate at electrical magnetic field ----- | 35 |
| Figure 1.2. Fundamental procedures of early modified ferric precipitation of ammonia nitrogen ----- | 76 |
| Figure 3.1. Relationship between ORP value of the suspension and oxidation time at different temperature ----- | 40 |
| Figure 3.2. Relationship between ORP value of the suspension and oxidation time at different pH value ----- | 42 |
| Figure 3.3. Relationship between ORP value of the suspension and oxidation time at different amount of air flow ----- | 43 |
| Figure 3.4. Effect of oxidation time on settling height rate of precipitates obtained at different temperature ----- | 46 |
| Figure 3.5. Effect of oxidation time on settling height rate of precipitates obtained at different pH value ----- | 48 |

LIST OF FIGURES

| | |
|--|----|
| Figure 1.1. Layer-by-layer illustration of the spinel structure | 6 |
| Figure 1.2. Oxygen ions of the spinel structure | 8 |
| Figure 1.3. A sites of the spinel structure | 9 |
| Figure 1.4. B sites of the spinel structure | 10 |
| Figure 1.5. Two subcells of a unite cell of the spinel structure | 11 |
| Figure 1.6. Main procedures of general ferrite process to treat waste water | 22 |
| Figure 1.7. Oxidation conditions for the formation of Fe_3O_4 | 26 |
| Figure 1.8. Eh-pH equilibrium diagrams at 25°C for the $\text{Fe}-\text{FeSO}_4\text{-X-H}_2\text{O}$ system | 31 |
| Figure 2.1. Schematic diagram of apparatus used in precipitation experiments at high temperature | 34 |
| Figure 2.2. Schematic diagram of measuring settling height rate of precipitate at electrical magnetic field | 35 |
| Figure 2.3. Experimental procedures of new modified ferrite precipitation at ambient temperature | 36 |
| Figure 3.1. Relationship between ORP value of the suspension and oxidation time at different temperature | 40 |
| Figure 3.2. Relationship between ORP value of the suspension and oxidation time at different pH value | 42 |
| Figure 3.3. Relationship between ORP value of the suspension and oxidation time at different amount of air flow | 43 |
| Figure 3.4. Effect of oxidation time on settling height ratio of precipitates obtained at different temperature | 46 |
| Figure 3.5. Effect of oxidation time on settling height ratio of precipitates obtained at different pH value | 48 |

| | |
|---|----|
| Figure 3.6. Effect of oxidation time on settling height ratio of precipitates obtained at different amount of air flow----- | 49 |
| Figure 3.7. Effect of oxidation time on settling height ratio of precipitates obtained with or without Fe_3O_4 seed ----- | 51 |
| Figure 3.8. Effect of aging time on the settling height ratio of precipitate obtained at room temperature ----- | 52 |
| Figure 3.9. Effect of aging time on the settling height ratio of precipitate obtained at room temperature with Fe_3O_4 seed ----- | 53 |
| Figure 3.10. Effect of aging time on the settling height ratio of precipitate obtained at 70°C ----- | 54 |
| Figure 3.11 (a). Standard X-ray power diffraction pattern of Fe_3O_4 , Cu-K α ----- | 56 |
| Figure 3.11 (b). X-ray powder diffraction of precipitate obtained at room temperature with the strongest magnetic property, Cu-K α ----- | 57 |
| Figure 3.11 (c). X-ray powder diffraction of precipitate obtained at room temperature after ORP abrupt change, Cu-K α ----- | 58 |
| Figure 3.12. TEM micrograph of precipitate obtained at room temperature with the strongest magnetic property ----- | 59 |
| Figure 3.13. Effect of oxidation time on settling height ratio of precipitates obtained from Noranda Tailing Water ----- | 62 |
| Figure 3.14. Magnetization curve of precipitate obtained from ferrite coprecipitation of Noranda Tailing Water ----- | 63 |
| Figure 3.15. X-ray powder diffraction of precipitate obtained from ferrite coprecipitation of Noranda tailing Water, Cu-K α ----- | 64 |
| Figure 3.16. TEM micrograph of precipitate obtained from ferrite coprecipitation of Noranda Tailing Water ----- | 65 |

| | |
|---|----|
| Figure 3.17. SEM energy dispersive analysis of precipitate obtained from ferrite coprecipitation of Noranda Tailing Water | 67 |
| Figure 3.18. Effect of oxidation time on settling height ratio of precipitates after 24hr aging obtained from Berkeley Pit Water | 69 |
| Figure 3.19. Effect of oxidation time on settling height ratio of precipitates after 48hr aging obtained from Berkeley Pit Water | 70 |
| Figure 3.20. Magnetization curve of precipitate obtained from ferrite coprecipitation of Berkeley Pit Water, (a) Fe/M molar ratio: 2 | 72 |
| Figure 3.20. Magnetization curve of precipitate obtained from ferrite coprecipitation of Berkeley Pit Water, (b) Fe/M molar ratio: 3 | 73 |
| Figure 3.20. Magnetization curve of precipitate obtained from ferrite coprecipitation of Berkeley Pit Water, (c) Fe/M molar ratio: 5 | 74 |

1. Introduction

Acid mine drainage is the largest environmental problem facing the mining and mineral processing industry today[1-3]. Acid mine drainage contains a high concentration of iron and other dissolved metals and has an excessively acidic pH. Chemical precipitation is the most common method to treat industrial and mining waste effluent. Ferrite precipitation is a novel method of treating heavy metal ions present in contaminated waste water. The ferrite sludge is stable and can be separated by magnetic separation, and the ferrite precipitate can be used as low cost magnetic material. Because ferrite precipitation is usually processed at a higher temperature, it is necessary to develop the ferrite precipitation at ambient temperature in order to treat the large quantities of acid mine drainage.

1.1. Acid Mine Drainage

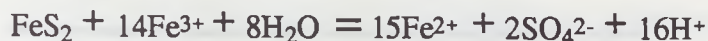
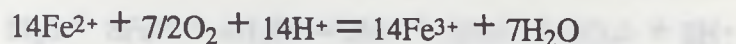
1.1.1. The formation of acid mine drainage

Most coal, shale, base metal, precious metal and uranium mines contain sulphide minerals, either in the ore or the surrounding waste rock and tailings. When these sulphide minerals, particularly pyrite and pyrrhotite, are exposed to oxygen and water, they begin to oxidize almost immediately. In the absence of calcareous materials, the initial chemical reactions produce acid and the acid solubilizes the heavy metals present in the waste rock and tailings.

In the case of pyrite, FeS_2 , the critical mineral, the reactions [4] are:

Direct pathway:

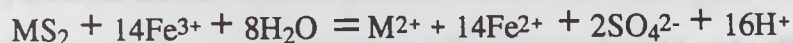


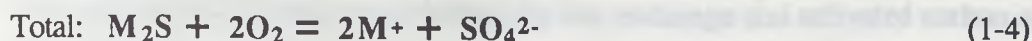
Indirect pathway:

For other metal sulfides (M_2S , MS or MS_2):



1.1.2 Treatment and waste handling





Bacteria can greatly increase the rate of oxidation [5]. Other metal impurities will also be dissolved by the acidic waste water formed from metal sulfides.

Acid mine drainage may contain very high concentrations of sulfate and Fe, high concentrations of metals such as Mg, Mn, Zn, Cu, Ni, Pb, Cd, etc., and exhibit acidic pH values. If acid mine drainage is left untreated, the drainage could eventually contaminate groundwater and local watercourses, damaging the health of plants, wildlife, and fish.

1.1.2. Treatment of acid mine drainage

At present, there are several methods in effect to treat acid mine drainage [1-7]. The most common method is chemical precipitation.

For chemical precipitation, the conventional approach has been lime neutralization to precipitate the metal hydroxides. The precipitated hydroxides are difficult to filter and metal hydroxides are not valuable product. Further, the metal hydroxides are not chemically stable. As a result, they are impounded as "hydroxide sludge" and will probably need to be decontaminated in the future.

The other precipitation technique which utilizes sulfides as precipitating agent, produces metal sulfides which are more stable as compared to hydroxides. Although it is difficult to filter the metal sulfides from solution, flotation can be used to separate most of the metal sulfides. For effective flotation separation, some environmentally toxic chemical

reagents are required, and complete removal by flotation is probably impossible. Under some circumstances when an excess of sodium sulfide is used as a precipitating agent, a hazardous gas H_2S is often produced during the precipitation. A closed reactor vessel with secure venting would be required to minimize safety risk.

In addition to these two chemical precipitation techniques, the removal of metal ions from the solution is also accomplished by ion exchange and activated carbon adsorption, which are expensive. Further, the adsorbed metals present in the loaded resins and carbon do not have any intrinsic value.

The utilization of ferrite precipitation process to treat waste water was initiated in the 1970's [8]. Ferrite precipitation was first developed for the manufacture of high quality magnetic materials. Once it was noticed that most of the heavy metal ions were incorporated into ferrite precipitates during the ferrite precipitating processes, the ferrite coprecipitation technique was applied to the treatment of heavy metal ions contaminated wastewater. At the present time, this technology has been applied to the treatment of waste waters such as laboratory waste water, industrial waste water, and others. The advantages of ferrite precipitation in comparison to other chemical precipitation techniques are [9] (1) simultaneous treatment of various kinds of heavy metal ions; (2) precipitates (ferrite particles) have chemical stability with little risk of redissolution; (3) filtration is easy and magnetic separation is possible; (4) divalent iron compound (ferrous sulfate, ferrous chloride, etc) which are added during the coprecipitation process are readily available as industrial wastes and as by-products from the iron and titanium industries; and (5) precipitates, such as spinel ferrite by-products, are used as low cost magnetic materials.

1.2. Ferrites and Their Applications

Ferrites are the most important ferrimagnetic substances which fall mainly into two groups with different crystal structures [10-12]:

1. Cubic ferrite These have the general formula $MO \cdot Fe_2O_3$ where M is a divalent metal ion, like Mn, Ni, Fe, Co, Mg, Zn, Cu, etc. or a mixture of more than one of these elements, and Fe^{3+} may be replaced by Fe^{3+} in combination with other trivalent ions. They are spinel ferrite because their crystal structure is very similar to that of the mineral spinel $MgO \cdot Al_2O_3$. Another kind of cubic ferrite is garnets that have a general formula $(M_2O_3)_3(Fe_2O_3)_5$ where M is trivalent metal such as yttrium or a rare earth metal, or a mixture of more than one of these. All cubic ferrites except for cobalt ferrite $CoO \cdot Fe_2O_3$, are magnetically soft or easily magnetized in a small field.

2. Hexagonal ferrite The hexagonal ferrites are a group of ferromagnetic oxides in which the principal component is Fe_2O_3 in combination with a divalent oxide of Ba, Sr, Pb, and a divalent transition metal oxide. The most important in this group is barium ferrite $BaO \cdot 6Fe_2O_3$ which is magnetically hard and referred to as permanent magnets.

1.2.1. Crystal structure of spinel ferrite

The spinel ferrite $MO \cdot Fe_2O_3$ is the most widely used ferrite. The presence of Fe^{+3} , Mn^{+2} , Ni^{+2} , Fe^{+2} , Co^{+2} can be used to provide the unpaired electron spins and therefore part of the magnetic moment of a spinel. Other divalent ions such as Mg^{+2} and Zn^{+2} (or monovalent Li^{+}) are used to disproportionate the Fe^{+3} ions on the crystal lattice sites to provide or increase the magnetic moment.

The crystal structure of the spinel ferrites is face-centered cubic, in that there are 8 "molecules" or a total of $8 \times 7 = 56$ ions, per unit cell. The layer-by-layer illustration of the spinel structure is shown in Figure 1.1.

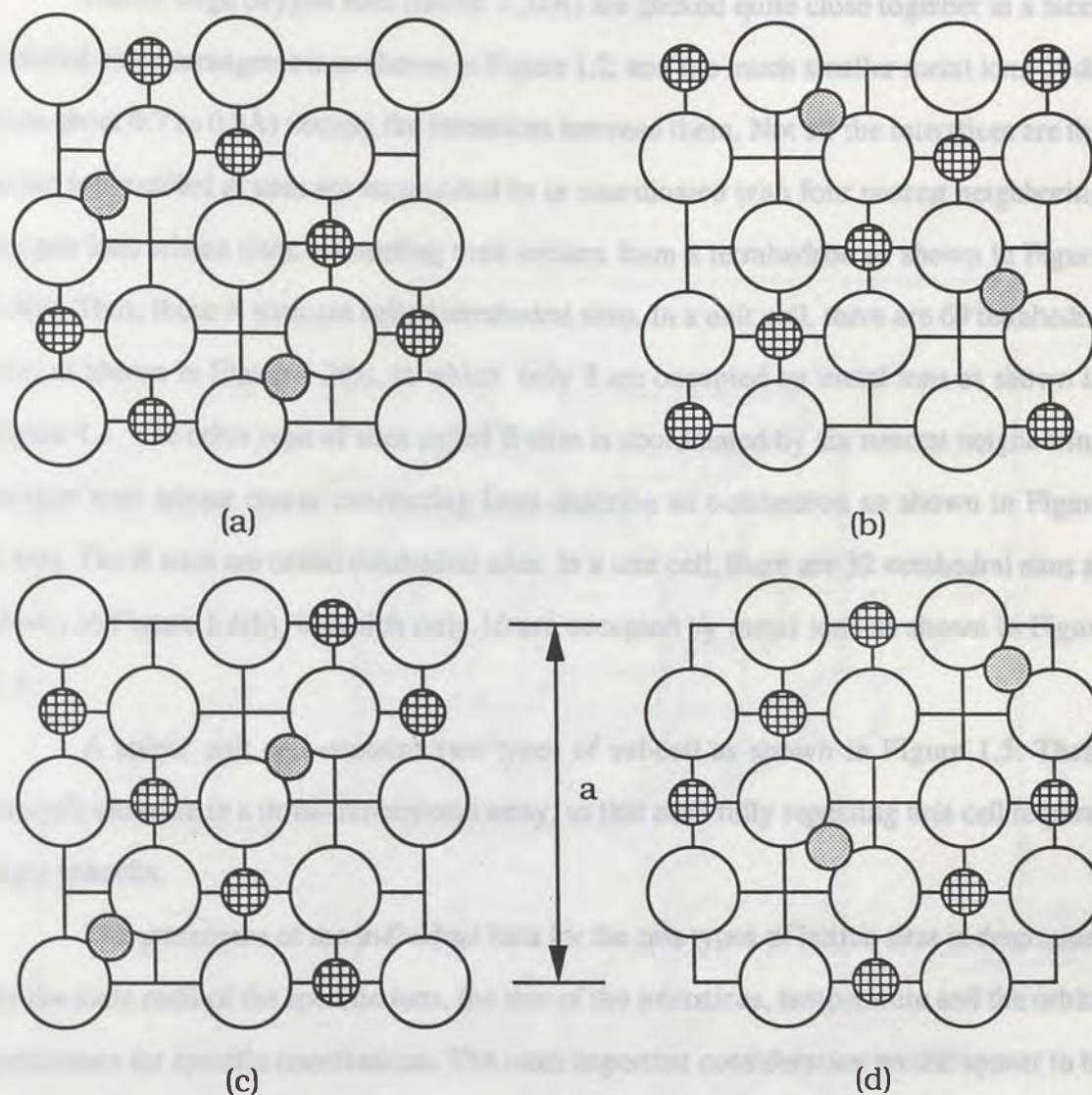


Figure 1.1. Layer-by-layer illustration of the spinel structure. The diagram shows the four layers that make up a unit cell of lattice parameter a . Successive layers are separated by a vertical distance $1/4 a$.



Oxygen ions



Metal ions in tetrahedral A site which are at a height $1/8 a$ above each layer



Metal ions in octahedral B site

The 32 large oxygen ions (radius 1.32\AA) are packed quite close together in a face-centered cubic arrangement as shown in Figure 1.2, and the much smaller metal ions (radii from about 0.7 to 0.8\AA) occupy the interstices between them. Not all the interstices are the same; some called A sites are surrounded by or coordinated with four nearest neighboring oxygen ions whose lines connecting their centers form a tetrahedron as shown in Figure 1.3(a). Thus, these A sites are called tetrahedral sites. In a unit cell, there are 64 tetrahedral sites as shown in Figure 1.3(b), in which only 8 are occupied by metal ions as shown in Figure 1.1. The other type of sites called B sites is coordinated by six nearest neighboring oxygen ions whose center connecting lines describe an octahedron as shown in Figure 1.4(a). The B sites are called octahedral sites. In a unit cell, there are 32 octahedral sites as shown in Figure 1.4(b), in which only 16 are occupied by metal ions as shown in Figure 1.1.

A spinel unit cell contains two types of subcell as shown in Figure 1.5. These subcells alternate in a three-dimensional array, so that each fully repeating unit cell requires eight subcells.

The preference of the individual ions for the two types of lattice sites is determined by the ionic radii of the specific ions, the size of the interstices, temperature and the orbital preference for specific coordination. The most important consideration would appear to be the relative size of the ion compared to the size of the lattice site. The divalent ions are generally larger than the trivalent. The octahedral sites are also larger than the tetrahedral. Therefore, it would be reasonable that the trivalent ions such as Fe^{+3} would go into the tetrahedral sites and the divalent ions would go into the octahedral. Two exceptions are found in Zn^{+2} and Cd^{+2} which prefer tetrahedral site because the electronic configuration is favorable for tetrahedral bonding to the oxygen ions.

If the M^{+2} are in A sites and Fe^{+3} in B sites, it is called the normal spinel structure. Both zinc and cadmium ferrite have this structure and they are both nonmagnetic, i.e.,

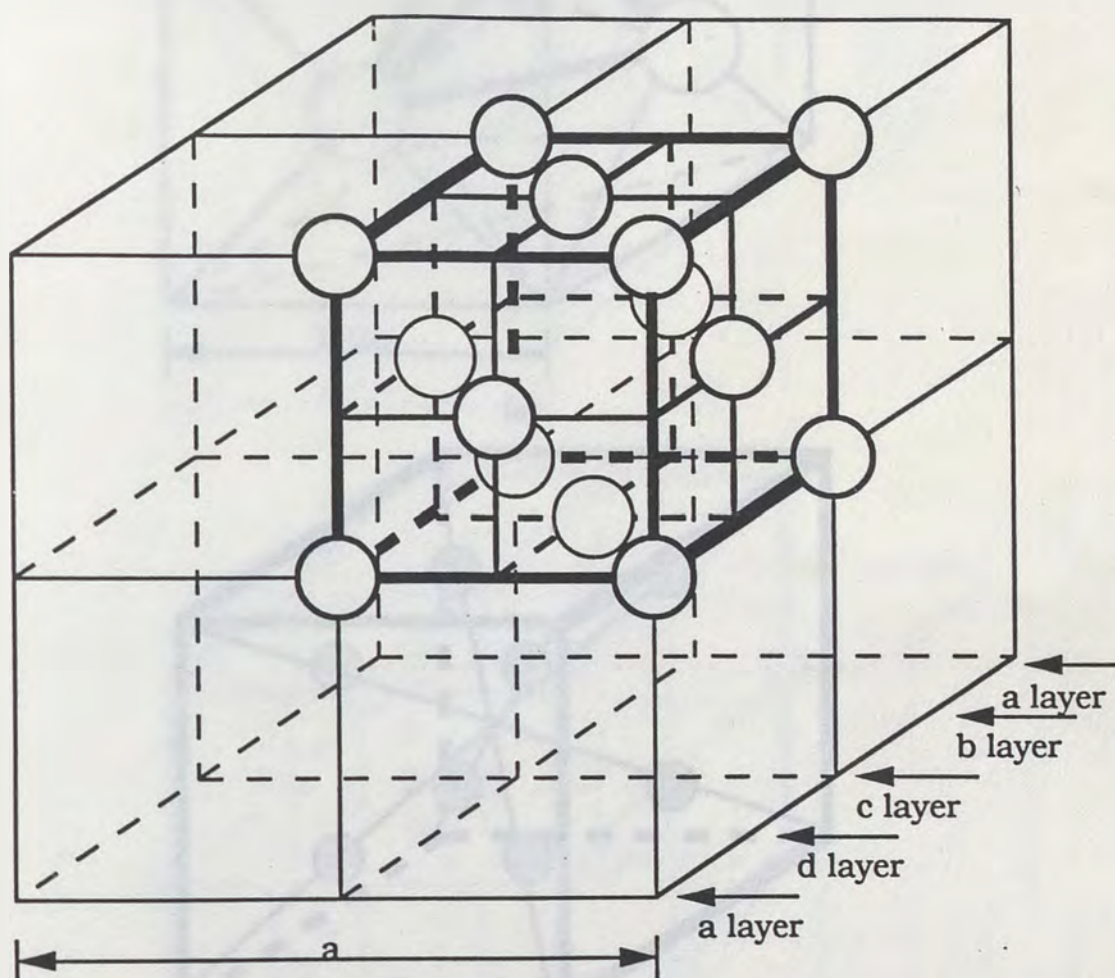
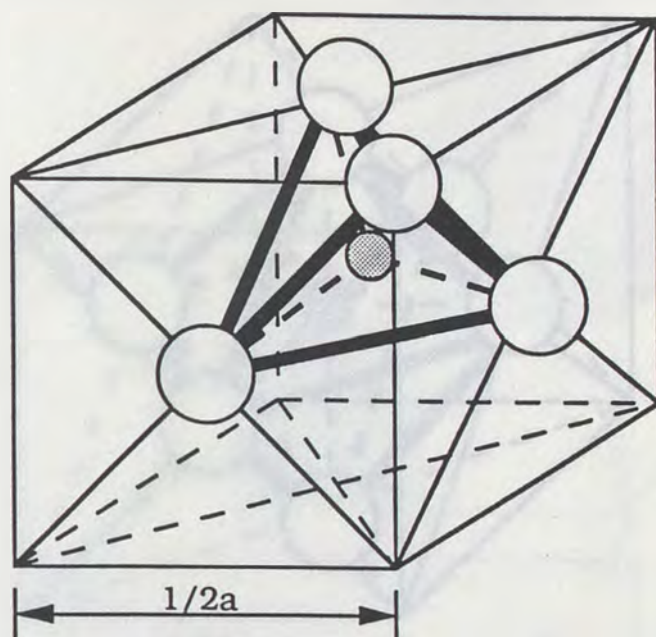
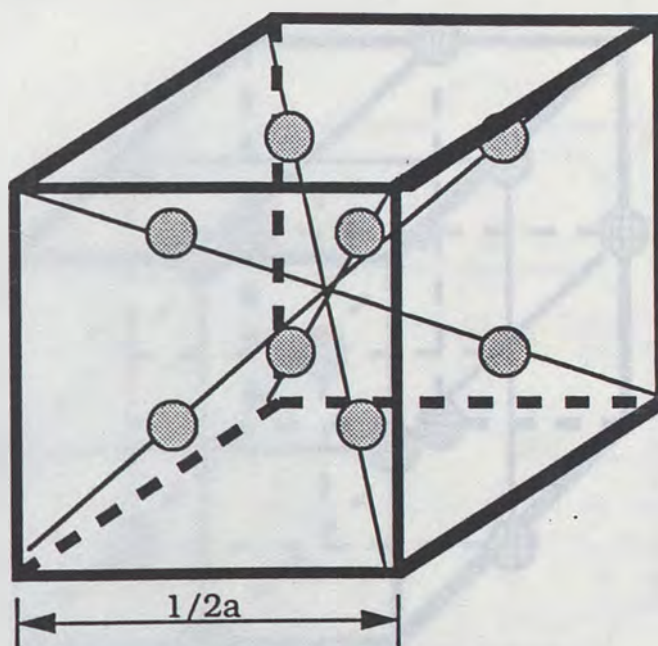


Figure 1.2. Oxygen ions of the spinel structure. The diagram shows the 1/8 unit cell of lattice parameter a . There are 32 oxygen ions in a unit cell.



(a)



(b)

Figure 1.3. (a) Tetrahedral A site, (b) Tetrahedral A sites of the spinel structure. The diagram shows the $1/8$ unit cell of lattice parameter a . There are 64 A sites in a unit cell and only 8 are occupied by metal ions

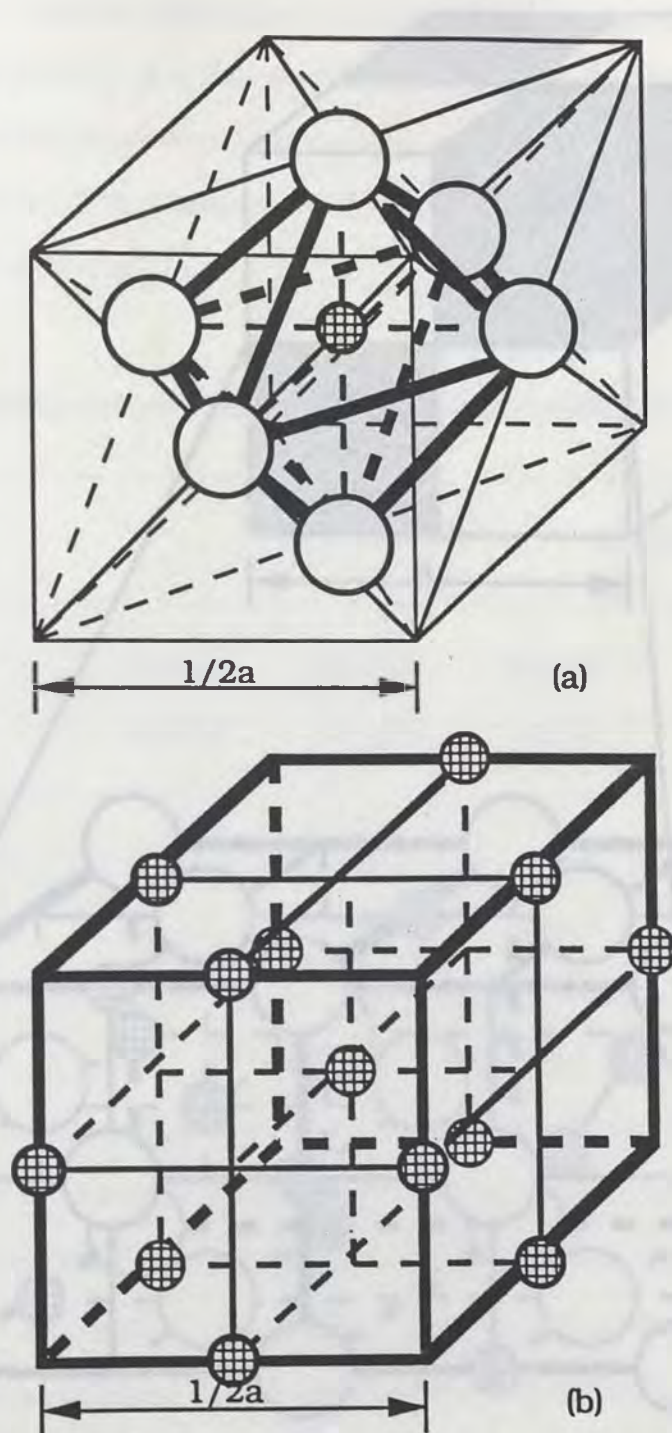


Figure 1.4. (a) Octahedral B site, (b) Octahedral B sites of the spinel structure. The diagram shows the $1/8$ unit cell of lattice parameter a . There are 32 B sites in a unit cell and only 16 are occupied by metal ions.

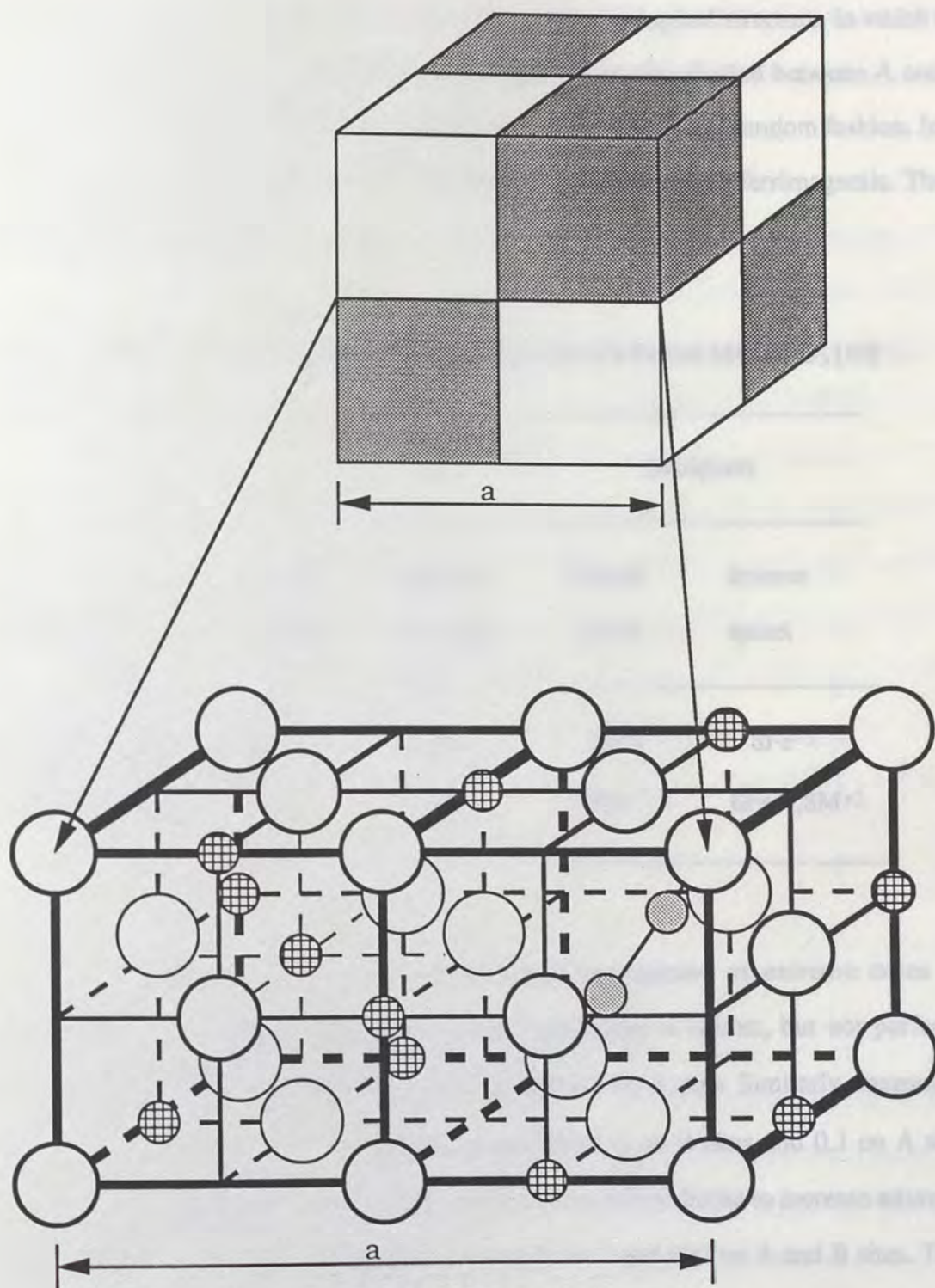


Figure 1.5. Two subcells of a unit cell of the spinel structure.

paramagnetic. However, Many other ferrites have the inverse spinel structure, in which the divalent ions are on B sites, and the trivalent ions are equally divided between A and B sites. The divalent and trivalent ions normally occupy the B sites in a random fashion. Iron, cobalt, and nickel ferrites have the inverse structure, and they are all ferrimagnetic. These are all shown in Table 1.1.

Table 1.1. Arrangements of Metal Ions in the Unit Cell of a Ferrite $MO \cdot Fe_2O_3$ [10]

| Kind of site | Number available | Number occupied | Occupants | |
|----------------|---------------------|--------------------|------------------|---------------------|
| | | | Normal spinel | Inverse spinel |
| Tetrahedral(A) | 64 | 8 | $8M^{+2}$ | $8Fe^{+3}$ |
| Octahedral (B) | 32 | 16 | $16Fe^{+3}$ | $8Fe^{+3}, 8M^{+2}$ |

The normal and inverse structures are to be regarded as extreme cases and intermediate structures can exist. Thus manganese ferrite is almost, but not perfectly, normal; a fraction 0.8 of the Mn^{+2} is on A sites and 0.2 on B sites. Similarly, magnesium ferrite is not quit inverse; a fraction 0.9 of the Mg^{+2} is on B sites and 0.1 on A sites. Besides, nonmagnetic zinc ferrite is often added to form mixed ferrite to increase saturation magnetization because Zn^{+2} changes the fraction of Fe^{+3} and M^{+2} on A and B sites. Table 1.2. gives the saturation magnetization and lattice parameter of some ferrites [10,12].

Finally, it should be noted that ferrites can be prepared containing two or more

different kinds of divalent ions, e.g., $(M_1, M_2, \dots)O \cdot Fe_2O_3$. This is called a mixed ferrite. The ratio of the divalent ions is depend on the method of preparation and application.

Table 1.2. Saturation Magnetization and Lattice Parameter of some Ferrites [10,12]

| Ferrite | Lattice Parameter(Å) | Saturation Magnetization(emu/g) | |
|---|-------------------------|---------------------------------|------|
| | | 0°K | 20°C |
| MnO·Fe ₂ O ₃ | 8.50 | 112 | 80 |
| FeO·Fe ₂ O ₃ | 8.39 | 98 | 92 |
| CoO·Fe ₂ O ₃ | 8.38 | 90 | 80 |
| NiO·Fe ₂ O ₃ | 8.34 | 56 | 50 |
| CuO·Fe ₂ O ₃ (quenched) | 8.37 | 30 | 25 |
| MgO·Fe ₂ O ₃ | 8.36 | 31 | 27 |
| ZnO·Fe ₂ O ₃ | 8.44 | 0 | 0 |

1.2.2. Conventional ferrite processing and applications [12]

Conventional ferrite processing includes powder preparation and sintering. A larger majority of ferrite powders are made by the conventional ceramic process. Firstly, raw materials that include oxides, carbonates, oxalates and nitrides which the last three compounds can be decomposed to oxides by heat treatment are selected. Then, raw materials are weighted, blended, milled, calcined and milled again. Finally, ferrite powders are die-pressed to the required shape to be sintered.

Non-conventional processes involve producing by a wet method like coprecipitation. Non-conventional powder can then be treated similarly to conventionally produced powder.

Ferrites are used in applications from simple lifting magnets to the most complex microwave communications to outer space because ferrite materials possess very wide properties. The permanent magnet consumes the greatest tonnage of ferrite which is mostly used in consumer items such as small motors for automotive and portable appliances or audio speakers. Permanent magnet ferrites are called hard ferrites as compared to soft ferrites which are used in telecommunications or power applications.

The largest use of soft ferrite is ferrite inductors and transformers in power application. In the early days of ferrites use, industry employed ferrites at extremely low power levels because the major application at that time was in telecommunications. The rapid growth of ferrites for high-power applications occurred because the rapid growth of computers and microprocesses require small, efficient power supplies that can be constructed with power ferrite components with low losses at higher frequencies and elevated power levels.

The other important application of ferrites is in microwave devices because of the absorption of energy by ferrites at microwave frequencies. Ferrites have also been used in magnetic recording which is the most important method of storing large amounts of information for computers as well as audio and video entertainment systems. In addition to the above applications of ferrites, other uses of ferrites take advantage of a combination of properties that are somewhat unique to ferrites like magnetostrictive transducers and sensors. Ferrites are also used as copier powders and ferrofluids, etc.

1.2.3. Applications of by-product ferrite

Much by-product ferrite is produced in mineral processing, such as in the mining

and purifying process for iron and titanium [13]. The by-product ferrite is also produced in the treatment of waste water contaminated by heavy metal ions, precipitated as ferrite compounds [8,9]. In order to recycle the by-product ferrite, several applications have been developed.

Magnetic-Marker System A typical application of the by-product is a magnetic-marker sensing system, which consist of a magnetic marker, made of the ferrite by-product, and a highly sensitive magnetic sensor, for detecting the position of the marker [9,13,14]. The by-product ferrite was formed into magnetic markers by mixing with resin, which contains more than 75wt% ferrite. By selecting a pertinent resin, it is easy to obtain markers in various forms such as rigid block, a flexible materials, or a thermally paintable film. From an economic viewpoint, the high-quality ferrite material used in electronics is impractical as magnetic markers because of the large volume requirement. With the ferrite by-product, the magnetic-marker system has been applied to a guide system for blind people to walk safely, and to automated guided vehicle system in factories and golf courses. This system is economical, due to recyclability of the by-product, and maintenance-free, without the disconnection problems that may occur in conventional guide systems using electric cables. It is also highly reliable, and require no electric power in the guide liner.

Vibration-Damping Materials With an increase of industrial activity, vibration and noise coming from various vehicles and machines have became serious pollution problem in our environment [9,15]. In some field of technology, even minimal mechanical noise should be avoided, to achieve good yield from production. Newly developed ferrite-resin composite materials using the ferrite by-product are effective for suppressing mechanical noise and vibrations. The mechanical damping material which is made by mixing ferrite grains and a resin, followed by compacting have relatively high rigidity and high damping properties. These materials are now being used for vibration and noise suppression in such

cases as the microfabrication of LSIs; the assembly of precision machines; inspection and measurement by powerful microscopes or electron microscopes; housings of audio equipment, computer peripherals and terminals; and supplementary construction materials for vehicles and ships.

Microwave Absorber Application Ferrite is a well know microwave-absorbing material [9,16,17]. Compared with high-dielectric material, ferrite absorbs a wider frequency band of microwaves with thinner materials. To avoid microwave reflection on the surface of electronic devices or leakage from electronic-oven home appliances, ferrite absorber is used; but this is limited to small sections of the equipment, because of cost limitations. Ferrite by-product, inexpensive and in abundant supply, facilitates larger-scale microwave-absorption engineering work, which was previously impossible due to the high cost. Ferrite by-product is mainly used for GHz-range microwave absorbers by mixing the ferrite and other required material with rubber or resin. As the microwave absorber has many outdoor use advantages, such as thin sheet configuration, good flexibility, and good weather durability, it has been applied for the suppression of radar ghosts caused by large iron bridges, ship masts, and for noise suppression of satellite-communication antennas and for other similar purposes.

Other Applications Ferrite particles have strong surface activity for absorbing harmful suspending matter on river-water surface as phosphates, algae, bacteria, etc. [9,18]. The water-pollution-control technique was proposed to make such materials absorb and coagulate onto ferrite particles and, finally, to separate, by means of an applied magnetic field. The use of ferrite by-product overcomes cost problems, and it is thus proposed as an economical and effective adsorbing material or scavenger.

Magnetic fluid, a mixture of fine ferrite particles and oil, is used to remove oil spills over water surfaces. The magnetic fluid is dispersed and spread over the water, and the oil, which becomes magnetic, is separated by means of a magnetic field. Magnetic fluid is also

used to separate nonferrous metal scraps.

1.3. Ferrite Precipitation

Ferrite precipitation originated from magnetic material research and the technique of manufacturing ferrite precipitates from aqueous solution was firstly established for high quality magnetic materials [19-21]. These high quality ferrites are made from precipitates having both the desired particle sizes and chemical compositions, which are obtained only by strictly controlling the precipitation conditions. These ferrites could not be easily produced by the conventional manufacturing technique, in which raw materials in the form of powders are mixed, presintered, formed and sintered.

1.3.1. Ferrite precipitation at high temperature

Since the first technique of ferrite precipitation from aqueous solution was established, many kinds of ferrites have been obtained by precipitation method. Manganese and cobalt ferrites [22] were prepared by the air oxidation of aqueous suspension of $\text{Fe}(\text{OH})_2$ and either $\text{Mn}(\text{OH})_2$ or $\text{Co}(\text{OH})_2$ at 50-80°C. In alkaline suspensions, all the metal ions are transformed into spinel ferrites, $\text{M}_x\text{Fe}_{3-x}\text{O}_4$ (M=Mn or Co), by suitable combination of the oxidation temperature and the concentration of the excess NaOH.

The formation of Mg-bearing ferrite by the air oxidation of aqueous suspensions was studied by Kaneko et al [23]. When the $\text{Mg}^{2+}/\text{Fe}_{\text{total}}$ molar ratio in the initial aqueous suspension is below 0.1 at pH 9.0 and 65°C, almost all Mg^{2+} is incorporated into the spinel type ferrite by the air oxidation of $\text{Fe}(\text{OH})_2$. At pH 8.0, a small amount of the Mg^{2+} is incorporated into the ferrite, between pH 9.0 and 10.0 only the Mg-bearing ferrite is formed, and at pH 11.0 the $\alpha\text{-FeO}(\text{OH})$ type compound is formed together with the Mg-

bearing ferrite.

The formation of Zn-bearing ferrite by air oxidation of aqueous suspension was studied by Kanzaki et al [26]. Zn-bearing spinel ferrites were obtained by air oxidation of the ferrous hydroxide suspension of the mole fraction Zn^{2+} to $[Zn^{2+}+Fe_{total}]$, r_{Zn} , ranging from 0.029 to 0.33 (except for 0.057) at pH 10.0 and 65°C, but at $r_{Zn} = 0.057$ only α -FeO(OH) was formed. The Zn-bearing spinel ferrite obtained at $r_{Zn}=0.33$ has the normal spinel structure. At pH 8.0, the Zn-bearing spinel ferrite is obtained at $r_{Zn}=0.57$, but the spinel ferrite is slightly oxidized to γ -Fe₂O₃.

The spinel CuFe₂O₄ ferrite by the precipitation method was developed by Pandya et al [28]. When both of the hydroxides, Cu(OH)₂ and Fe(OH)₂, were added to the solution of NaOH, simultaneous precipitation occurred and a suspension (pH=9.8) containing dark bluish green intermediate precipitates was formed. The suspension was then heated and kept at a temperature of 55°C while oxygen gas was bubbled uniformly into the suspension to stir it as well as to promote the oxidation reaction, until all the intermediate precipitates changed into the dark brownish precipitate of the spinel CuFe₂O₄.

In addition to above elements often present in waste water, the formation of Cd-bearing ferrite by the air oxidation of aqueous suspensions was also studied by Kaneko et al [24], lead-bearing ferrite by Tamaura et al [25], and molybdenum-bearing ferrite by Kanzaki et al [27].

Besides, the formations of multivalent metal ferrite with spinel structure have also been studied. The formation of the oxidized Fe₃O₄-Fe₂TiO₄ solid solution by the air oxidation of the aqueous suspension was studied by Katsura et al [29]. The formation of a chromium-bearing ferrite, Cr_{0.42}Fe_{2.56}O_{4.00}, in aqueous suspension by nitrate oxidation was studied by Tamaura et al [30]. The formation of aluminum-bearing ferrite in aqueous suspension by air oxidation was studied by Ito et al [31], and the formation of V-bearing

ferrite by aerial oxidation of an aqueous suspension was studied by Tamaura et al [32].

Further, the formations of various metals ferrite precipitate from aqueous suspensions were studied and the preparation of mixed metal ferrite like Mn-Zn ferrite by co-precipitation was also developed [20,33].

1.3.2. Ferrite precipitation at room temperature

Although all the above precipitates of spinel ferrites are obtained from an aqueous solution containing ferrous ions and the metallic ions by oxidation at a temperature above 50°C, various metal ferrites can also be precipitated at room temperature through forming some intermediate precipitates.

The formation of zinc(II)-bearing ferrites from γ -FeO(OH) was studied by Ito et al [34]. Stoichiometric zinc(II)-bearing ferrites were formed by increasing the reaction pH of a mixture of γ -FeO(OH), Fe(II), and Zn(II) ions to 9.0(25°C) and allowing it to stand for 60hrs. This reaction is initiated by the adsorption of the Fe(II) ion on γ -FeO(OH).

Cadmium(II)-, magnesium(II)-, and zinc(II)-bearing ferrites formed from γ -FeO(OH) at various reaction pH's were also studied by Ito et al [35]. The reaction of γ -FeO(OH) with the metal [Cd(II), Mg(II), or Zn(II)] and Fe(II) ions in solution gave the metal ion-bearing ferrites without oxidation. The Cd(II)- and Mg(II)-ion content in the ferrites increases with an increase in the reaction pH, but the Zn(II)-ion content is almost constant at pH 7.5-10.5, which agrees with that of the fractional adsorption of these metals on γ -FeO(OH). This suggests that only the adsorbed metal ions are incorporated into the ferrites.

Zn(II)- bearing green rust II and its spontaneous transformation into Zn(II)-bearing

ferrite in aqueous solution was studied by Tamaura [36]. When solution containing Fe(II), Zn(II), and SO_4^{2-} ions were oxidized by a mixed gas of air and nitrogen at pH 6.7 (25°C), a Zn(II)-bearing green rust II (GR-II), which is a uniform crystalline precipitate with a definite chemical composition, was formed. The molar ratio of Zn(II)/Fe(II) in the Zn(II)-bearing GR-II increased linearly with an increase in the Zn(II)/Fe(II) molar ratio in the reaction solution. The Zn(II)-bearing GR-II was spontaneously transformed into Zn(II)-bearing ferrite. In this reaction, Zn^{2+} ions in the Zn(II)-bearing GR-II are preferentially incorporated into the ferrites. Similar results were also obtained by Tamaura[37] in the study of Ni(II)-bearing green rust II and its spontaneous transformation into Ni(II)-bearing ferrites.

Tamaura et al [39] also studied that Zn(II)-, Cd(II)-, Ni(II)-, and Co(II)-bearing ferrites with spinel structure were synthesized from the intermediates (green rust II) that had been formed from $\gamma\text{-FeO(OH)}$ in aqueous suspensions. These intermediates were obtained when Fe(II) ion was added to the $\gamma\text{-FeO(OH)}$ suspension containing SO_4^{2-} and the metal ions at 25°C (pH 8.5). This reaction is considered to be initiated by the adsorption of Fe(II) ions to $\gamma\text{-FeO(OH)}$.

Tamaura [38] concluded two ferrite formation reactions in which no oxidants are used: (1) the transformation of $\gamma\text{-FeO(OH)}$ into ferrites and (2) the spontaneous transformation of the "green rust" into ferrites. They obtained the mixed ferrites, $\text{M}_x\text{Fe}_{3-x}\text{O}_4$ by allowing the following suspensions under an N_2 atmosphere for 2 to 60hrs in the pH range of 6.8 to 11 (20 to 90°C): (a) the $\gamma\text{-FeO(OH)}$ suspension containing Fe(II) and other metal ions M(II,III); and (b) the green rust suspension [the green-rust-II (GR-II) suspension, containing M(II), and the suspension of the "metal-ion-bearing green rust" (M-GR which contains metal ions M(II) in the lattice points of the GR)]. In these reactions,

some complexes composed of Fe(II), Fe(III), and M(II,III) formed in the dissolution step were spontaneously transformed into ferrites without any oxidation process. Since these processes do not need the oxidation process, no oxidation by-product such as α -FeO(OH), amorphous iron hydroxides, etc, are formed. The ferrite formed is extremely pure ferrite.

1.4. Ferrite Coprecipitation of Heavy Metals from Waste Water

From the foregoing description, it can be realized that the most of the heavy metal ions are incorporated into ferrite precipitates during coprecipitation. It is quite possible that heavy metal ions present in waste water can also be precipitated in the stable ferrite. Therefore, the ferrite coprecipitation technique has been applied to treat wastewater containing heavy metals e.g. laboratory wastewater, industrial wastewater and mine drainage.

1.4.1. General ferrite process for the treatment of waste water containing heavy metals [8,9,40-43]

First, wastewater was pretreated to remove oxygen by passing nitrogen. The required ferrous sulfate was added and then alkali like NaOH or Ca(OH)_2 was added to adjust the pH value to 9-11. The suspension is heated up to 50°C or higher and then oxidized by air. After oxidation, the ferrite sludge and clean water are separated by applying magnetic field. The procedure is schematically shown in Figure 1.6. The ferrite sludge is with high saturation magnetization [42,43] and the concentration level of heavy metals is lower than the regulations or the level to be determined. Table 1.3. shows concentrations of heavy metals in influent and effluent from laboratory wastewater [8].

Table 1.3. Concentration of Heavy Metals in Effluent

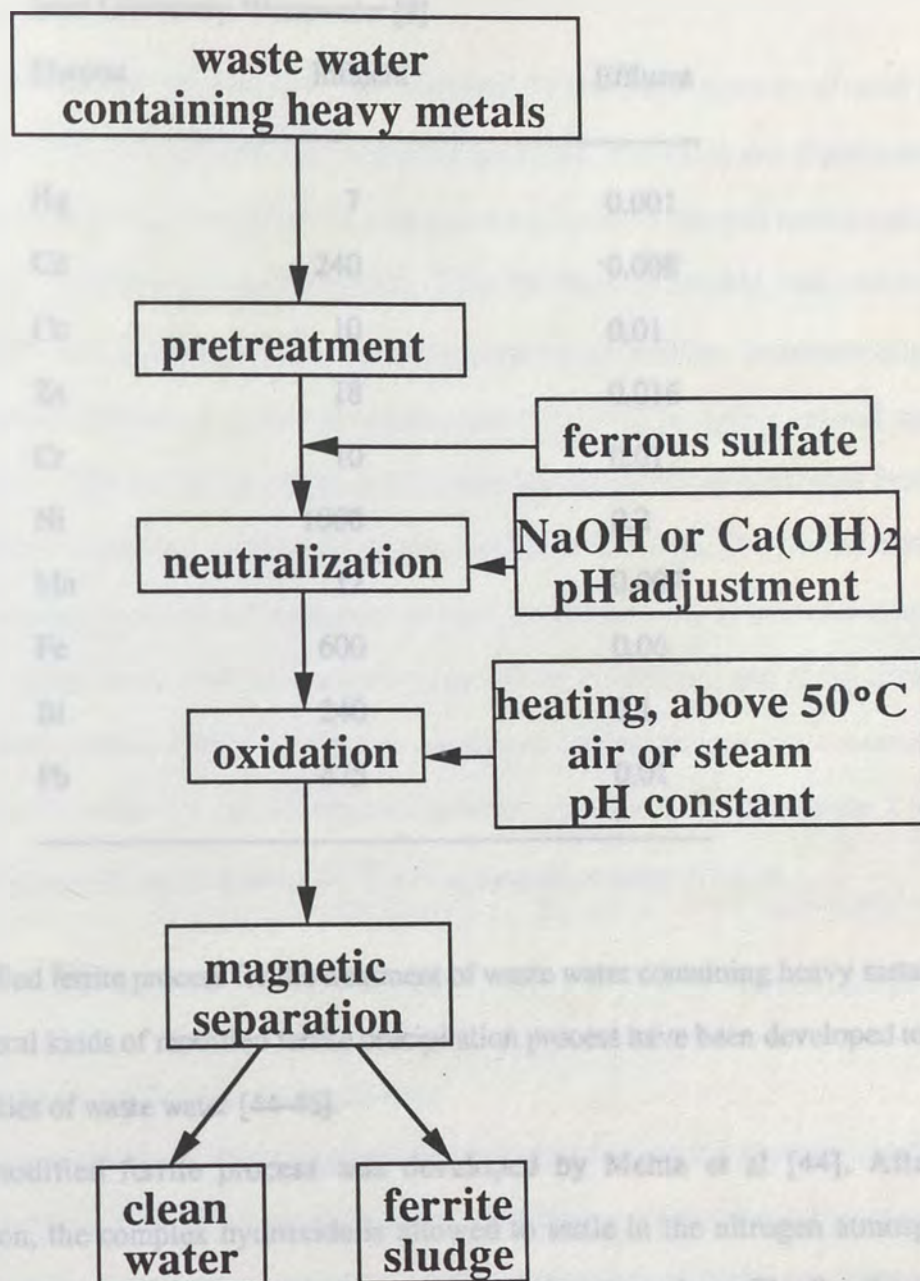


Figure 1.6. Main Procedures of General Ferrite Process to Treat Waste Water

Table 1.3. Concentrations(mg/l) of Heavy Metals in Influent and Effluent from Laboratory Wastewater [8]

| Element | Influent | Effluent |
|---------|----------|----------|
| Hg | 7 | 0.001 |
| Cd | 240 | 0.008 |
| Cu | 10 | 0.01 |
| Zn | 18 | 0.016 |
| Cr | 10 | 0.01 |
| Ni | 1000 | 0.2 |
| Mn | 12 | 0.007 |
| Fe | 600 | 0.06 |
| Bi | 240 | 0.1 |
| Pb | 475 | 0.01 |

1.4.2. Modified ferrite process for the treatment of waste water containing heavy metals

Several kinds of modified ferrite precipitation process have been developed to treat large quantities of waste water [44-46].

A modified ferrite process was developed by Mehta et al [44]. After the neutralization, the complex hydroxide is allowed to settle in the nitrogen atmosphere. Subsequently the sludge is heated at about 100°C in the atmosphere. Finally, the sludge was diluted followed by magnetic separation.

A ferrite process using powder magnetite as a promoter to keep the treatment temperature at the ambient level was developed by Ito et al [45]. Magnetite powder 0.3g/l or more was added to the water containing 20mg/l heavy metals and molar ratio of

$\text{Fe}^{2+}/\text{M}(\text{M: heavy metal})=12$ as a promoter, and then the ferrite process was performed at low temperature (0-25°C).

The process for recovering ferrite materials from a large quantity of acid mine drainage containing iron ions was developed by Sano [46]. The silica and aluminum free ferric hydroxide was recovered from the drainage water by oxidation and neutralization in the pH region lower than 3.6, using CaCO_3 . Then the ferric hydroxide was mixed with ferrous sulfate and then the mixture is neutralized with $\text{Ca}(\text{OH})_2$. Subsequently, the mixture is allowed to stand at normal temperature (15-25°C) for aging several days to several weeks. After aging, the ferrite precipitates are magnetically separated from by-product gypsum or excess neutralization agents, CaCO_3 or $\text{Ca}(\text{OH})_2$. The characteristics of the ferrite material thus formed depend on reaction conditions such as iron concentration, mixture pH value, ferric- and ferrous-hydroxide mixing proportion, and aging time. The ferrite material produced by the optimum conditions having ferrous ion concentration 0.1 mol/L, $\text{Fe}^{3+}/\text{Fe}^{2+}$ ratio 1.7, pH 10, reaction solution quantity 1.7L, aging time 2 weeks, shows 25 m²/g specific surface area and 70 emu/g saturation magnetization.

1.5. Mechanism of ferrite precipitation

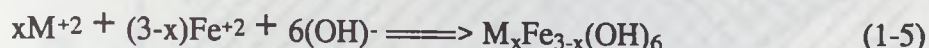
The mechanism of ferrite precipitation is dependent on the reaction conditions. Different conditions of ferrite precipitation have different mechanisms. Ferrous ferrite $\text{FeO}\cdot\text{Fe}_2\text{O}_3$ or Fe_3O_4 is a well-known ferrite. The mechanism of ferrite precipitation will mainly be that of ferrous ferrite.

1.5.1. Mechanism of Ferrite precipitation at high temperature

When divalent Fe ions, Fe^{2+} , coexist with non ferrous metal ions, M^{2+} , in an

aqueous solution, the addition of an equivalent amount of alkali will induce the following reaction [8,47,48]:

Neutralization



When this hydroxide is oxidized under a specific temperature and pH value, a spinel compound (ferrite) is formed according to the following reaction:

Oxidation



The reaction (1-6) is a overall reaction.

The optimum conditions for the formation of Fe_3O_4 by the air oxidation of $Fe(OH)_2$ suspensions were studied by Kiyama et al [47]. The suspensions obtained by mixing NaOH and $FeSO_4$ solutions in various values of $R(=2NaOH/FeSO_4)$ were subjected to oxidation with air at various temperatures. Figure 1.7. shows the conditions for the formation of Fe_3O_4 . The temperature of formation become low as R approaches 1.0. In neutral suspensions ($R < 1$), Fe_3O_4 is formed via green rust II or a mixture of green rust II and $Fe(OH)_2$. By further oxidation, the Fe_3O_4 formed gradually changes to $\gamma-Fe_2O_3$. A mixture of $\alpha-FeO(OH)$ and either $NaFe_3(OH)_6(SO_4)_2$ or $\alpha-Fe_2O_3$ is formed as the final oxidation product. In alkaline suspensions ($R > 1$), Fe_3O_4 is formed directly. The morphology and ferrous-ion content of Fe_3O_4 change considerably with the presence of green rust II before the formation of Fe_3O_4 . It suggested that Fe_3O_4 is formed near the surface of the particles of $Fe(OH)_2$ and green rust II by the coprecipitation of ferrous ions with ferric hydroxy-complexes.

To improve reaction conditions for the ferrite process, oxidation of the reactive

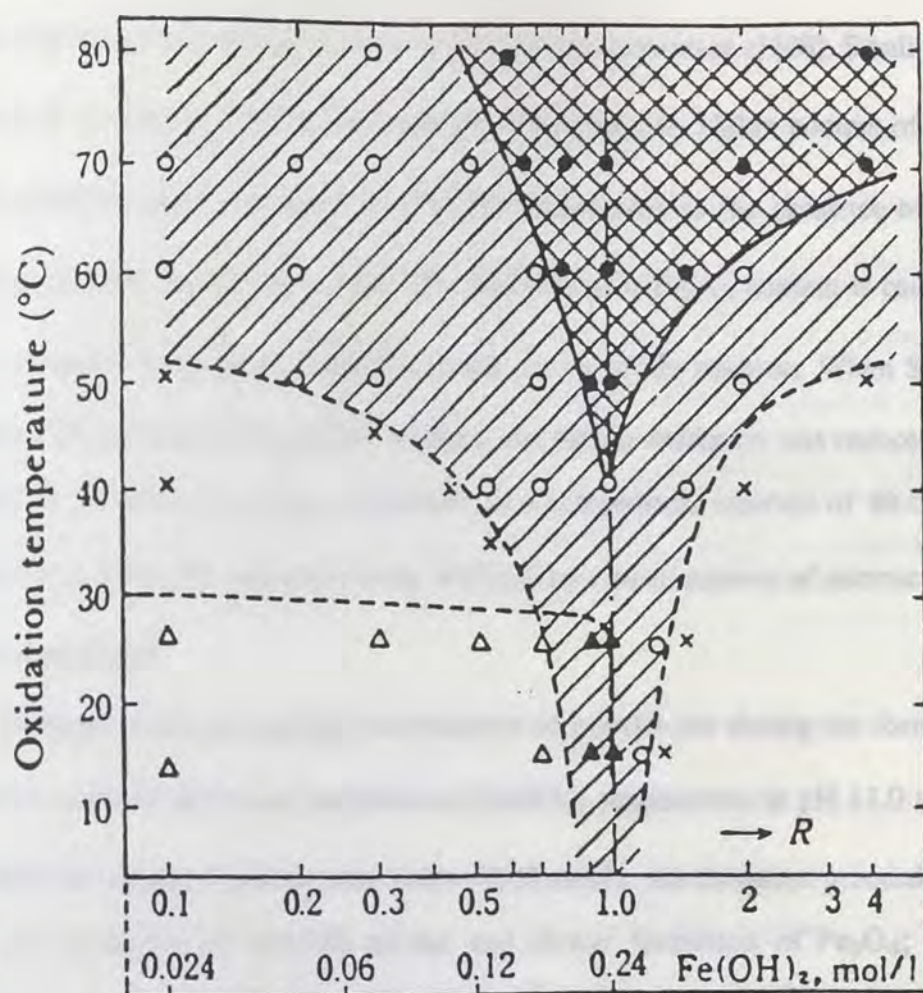


Figure 1.7. Oxidation Conditions for the Formation of Fe_3O_4 [47]

R : $2\text{NaOH}/\text{FeSO}_4$ molar ratio.

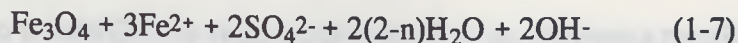
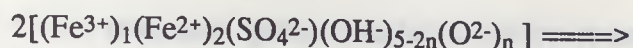
$\text{Fe}(\text{OH})_2$ mol/l: the amount of $\text{Fe}(\text{OH})_2$ in the starting suspension, calculated from the R value

- : Fe_3O_4
- x : $\alpha\text{-FeO}(\text{OH})$
- : A mixture of Fe_3O_4 and $\alpha\text{-FeO}(\text{OH})$
- ▲ : A mixture of Fe_3O_4 , $\alpha\text{-FeO}(\text{OH})$ and $\gamma\text{-FeO}(\text{OH})$
- △ : A mixture of $\alpha\text{-FeO}(\text{OH})$ and $\gamma\text{-FeO}(\text{OH})$

$\text{Fe}(\text{OH})_2$ suspension induced by sucrose was studied by Tamaura et al [48]. Small particles consisting of the Fe_3O_4 - γ - Fe_2O_3 solid solution having slightly higher content of γ - Fe_2O_3 were obtained by aerial oxidation of $\text{Fe}(\text{OH})_2$ suspension in the presence of a weak dispersing reagent, sucrose, at pH 9.0. The increase of γ - Fe_2O_3 content is caused by a further oxidation of the Fe_3O_4 particles in the course of the reaction. When SO_4^{2-} ion coexisted with sucrose in the reaction medium, the further oxidation was reduced and the treatment of the wastewater was improved. At a temperature interval of 40-65°C, the formation of α - $\text{FeO}(\text{OH})$ was completely inhibited by a small amount of sucrose and only Fe_3O_4 was obtained.

Tamaura et al also studied the oxidation of iron(II) ion during the formation of Fe_3O_4 and α - $\text{FeO}(\text{OH})$ by air oxidation of $\text{Fe}(\text{OH})_2$ suspensions at pH 11.0 and 65°C [49]. When the sulphate concentration is low (0.03 mol/l), the oxidation proceeds in three stages: (1) formation of iron(III) oxides and slower formation of Fe_3O_4 ; (2) rapid formation of Fe_3O_4 ; and (3) linear formation of Fe_3O_4 . When the sulphate concentration is high (0.60 mol/l), α - $\text{FeO}(\text{OH})$ is formed accompanied by a slow formation of amorphous γ - $\text{FeO}(\text{OH})$. The oxidation rates observed in the stationary state are due to the oxidation of Fe^{II} adsorbed on the surface of the solid phase.

Conditions for the synthesis of a pure green rust II with a definite chemical composition and its transformation reaction to Fe_3O_4 under a nitrogen atmosphere were studied by Tamaura et al [50]. The green rust II with the composition of $(\text{Fe}^{3+})_1(\text{Fe}^{2+})_2(\text{SO}_4^{2-})(\text{OH}^-)_{5-2n}(\text{O}^{2-})_n$ is spontaneously transformed in to Fe_3O_4 under a nitrogen atmosphere at 50-75°C according to the following reaction:

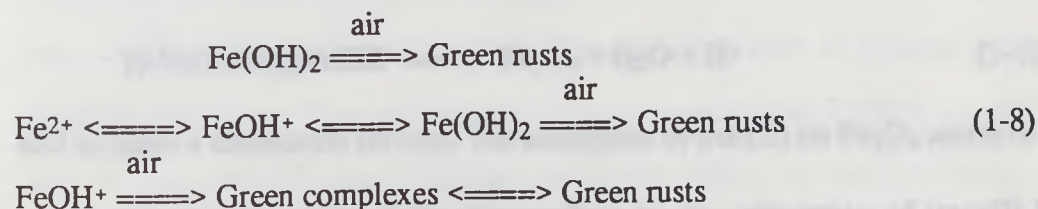


The transformation reaction is involved the dissolution process of the green rust II, some dissolved species such as the green complex II are released and transformed to Fe_3O_4 without being oxidized. The reaction pH affect the initial rates of the transformation reaction. The temperature and SO_4^{2-} also affect the rate. When temperature is lower, or SO_4^{2-} concentration is higher, the rate is slower. From the experimental evidence, they indicate that the green rust II can be transformed into Fe_3O_4 not only by oxidation but also spontaneously without oxidants.

1.5.2. Mechanism of ferrite precipitation at room temperature

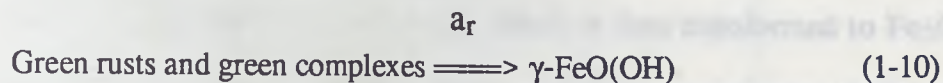
The mechanism of formation of iron oxide and oxyhydroxides in aqueous solutions at room temperature was studied by Bernal et al [51] and Misawa et al [52]. The mechanism related to the formation of Fe_3O_4 is introduced in this section.

When ferrous solution is treated with alkali under air-free condition, the white precipitate, $\text{Fe}(\text{OH})_2$, is formed. In the presence of air, it is rapidly changed to green precipitate, green rust I in chloride solution, or green rust II in sulphate solution. Green rusts is also obtained by the oxidation of ferrous ion. Green rusts are formed as follows:



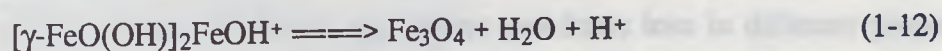
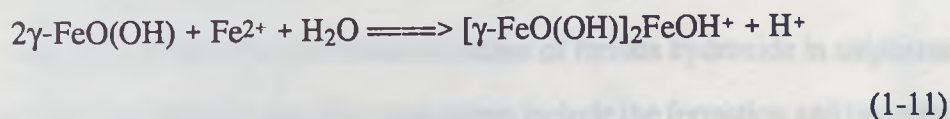
Once green complexes or green rusts is formed as intermediates, further oxidation is governed by its existence.

Green rusts and green complexes can be converted into Fe_3O_4 by slow aerial oxidation, a_s , and into $\gamma\text{-FeO(OH)}$ by rapid aerial oxidation, a_r , following reaction:



Fe_3O_4 can also be formed by the neutralization of mixed $\text{Fe(II)}_1\text{-Fe(III)}_2$ solutions.

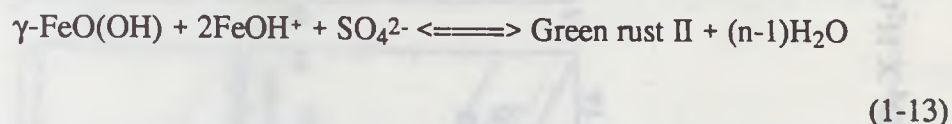
Then $\gamma\text{-FeO(OH)}$ can be converted to Fe_3O_4 at room temperature. Tamaura et al studied the transformation of $\gamma\text{-FeO(OH)}$ to Fe_3O_4 by adsorption of iron(II) ion on $\gamma\text{-FeO(OH)}$ [53]. When the pH of a reaction mixture of $\gamma\text{-FeO(OH)}$ and the iron(II) ion is raised from 5 to 9, the $\gamma\text{-FeO(OH)}$ is transformed to stoichiometric Fe_3O_4 at 25°C . The transformation reaction is triggered by the adsorption of the iron(II) ion on $\gamma\text{-FeO(OH)}$ at a pH above 7.3, and the adsorbed $\text{Fe}^{\text{II}}\text{-}\gamma\text{-FeO(OH)}$ is subsequently transformed to Fe_3O_4 . In each step, one proton is released, a total of two protons being released in the reaction. The reactions of the transformation steps are written as follows:



and includes a dissolution process. The adsorption of iron(II) on Fe_3O_4 seems to take place along with the formation of the intermediate by the adsorption of iron(II) ion on $\gamma\text{-FeO(OH)}$.

The mechanism of the transformation of $\gamma\text{-FeO(OH)}$ to Fe_3O_4 and/or green rust II

in an aqueous solution containing Fe^{II} ion in the presence or absence of the SO_4^{2-} ion at 298K is described by Tamaura et al [54]. $\gamma\text{-FeO(OH)}$ is dissolved by two molar of Fe^{II} ions adsorbed on the surface of $\gamma\text{-FeO(OH)}$, and a dissolved species (DS, $[(\text{Fe}^{2+})_2(\text{Fe}^{3+})(\text{OH}^-)_4(\text{O}^{2-})]^{1+}$) is formed, which is then transformed to Fe_3O_4 in the absence of SO_4^{2-} , or green rust II in SO_4^{2-} -containing suspension. The equilibrium reaction of the formation of green rust II from $\gamma\text{-FeO(OH)}$ is:



The equilibrium constant, K , is given by:

$$K = 1/(\text{FeOH}^+)^2[\text{SO}_4^{2-}]$$

or:
$$K = [\text{H}^+]/(K_h^2[\text{Fe}^{2+}]^2[\text{SO}_4^{2-}]), \quad K = 2.14 \times 10^8$$

where K_h is the hydrolysis constant of Fe^{2+} . This shows that, for a given proton concentration (pH), higher concentrations of Fe^{2+} and SO_4^{2-} ions facilitate the formation of green rust II from $\gamma\text{-FeO(OH)}$. When pH is high (pH 10), little green rust II is formed even at high SO_4^{2-} concentration, the DS is transformed to Fe_3O_4 .

Olowe et al [59-63] studied the oxidation of ferrous hydroxide in sulphated aqueous medium and also indicated that the mechanisms include the formation and transformation of intermediate compounds containing ferrous and ferric ions in different proportions at different conditions. They defined green rust II as green rust 2 (GR2) in acidic medium with higher ferrous ion, hydrated magnetite (HM) in stoichiometric condition $\text{FeSO}_4/\text{NaOH}=0.5$, pH 9-11) and other basic intermediated compounds in basic medium, and calculated Eh-pH equilibrium diagrams at 25°C for the Fe- FeSO_4 -X- H_2O system as shown in Figure 1.8. [63].

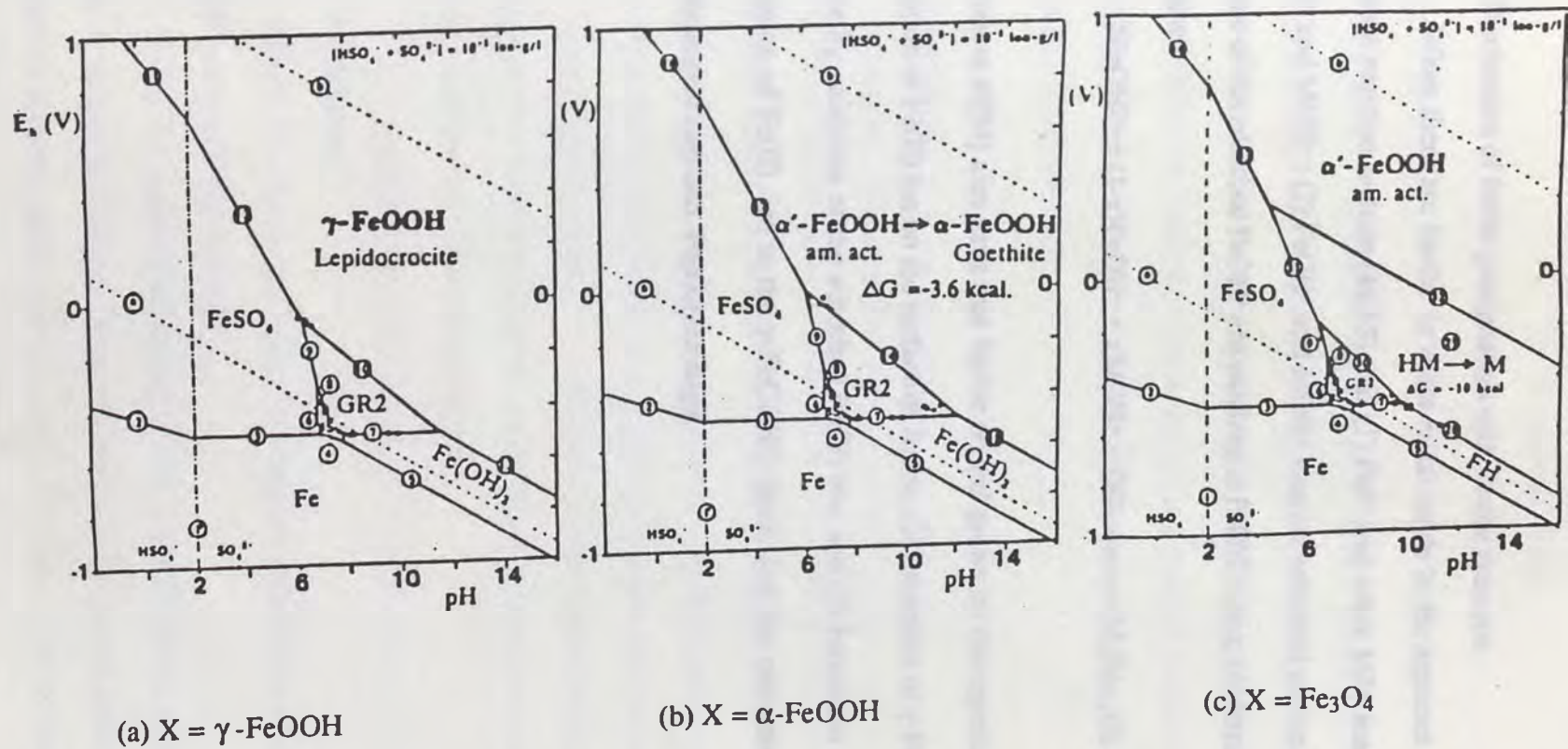


Figure 1.8. Eh-pH equilibrium diagrams at 25°C for the Fe-FeSO₄-X-H₂O system[63]

2. Experimental

1.5.3. Mechanism of ferrite precipitation with ferrite promoter

When there are ferrite or other metal oxide in the aqueous solution, the ferrite formation reaction include [45,55] that (1) Fe^{2+} and other M^{2+} ions are hydrolyzed to FeOH^+ and MOH^+ ; (2) FeOH^+ and MOH^+ ions are adsorbed on the oxide surface layer; (3) some of the adsorbed FeOH^+ are oxidized to FeOH^{2+} ions; (4) ferrite formation reaction as follow:



(1-14)

Tamaura et al[54] also gave that ferrite crystal grows by the repetition of 3 steps of (1) adsorption of Fe(II) ion on the surface of ferrite, (2) formation of $\gamma\text{-FeO(OH)}$ layer on the surface by oxidation of the adsorbed Fe(II) ion, and (3) formation of a ferrite layer by adsorption of Fe(II) ion to the $\gamma\text{-FeO(OH)}$ layer, and the rate-determining step is the transformation step into Fe_3O_4 (3rd step).

2. Experimental

2.1. Raw Materials

Deionized or distilled water was used in all the experiments. In this investigation, two different acid mine waters were used. One was Noranda Tailing Water that was prepared by leaching the Noranda Tailings (obtained from Quebec, Canada). The other one was the Berkeley Pit Water from Butte, Montana. Chemical grade $\text{FeSO}_4 \cdot 7\text{H}_2\text{O}$ obtained from Fisher Scientific was used. Chemical grade NaOH from Fisher Scientific was used to prepare 4M NaOH solution.

2.2. Apparatus

Oxidation The reaction vessel specially constructed for the air oxidation experiments at high temperature is shown as Figure 2.1. A flask fitted with 4 inlet holes was used. The temperature of the vessel was kept constant at $\pm 0.5^\circ\text{C}$ by a heating element at water bath. A platinum combination electrode or pH combination electrode was used to measure the ORP or pH of suspension. An air bubbler was used for air oxidation.

Magnetic Settling Rate Figure 2.2. is the schematic diagram of the magnetic settling apparatus used for settling rate measurements. These measurements will indicated the magnetic properties of the precipitate sludge.

2.3. Procedures

Figure 2.3. shows the main experimental procedures of new modified ferrite precipitation at ambient temperature.

Firstly, the required amount of ferrous sulfate was dissolved in 200ml deionized water, or acid mine drainage. Then 4M NaOH solution was added and pH value were adjusted to required value and the suspension was stirred at room temperature until

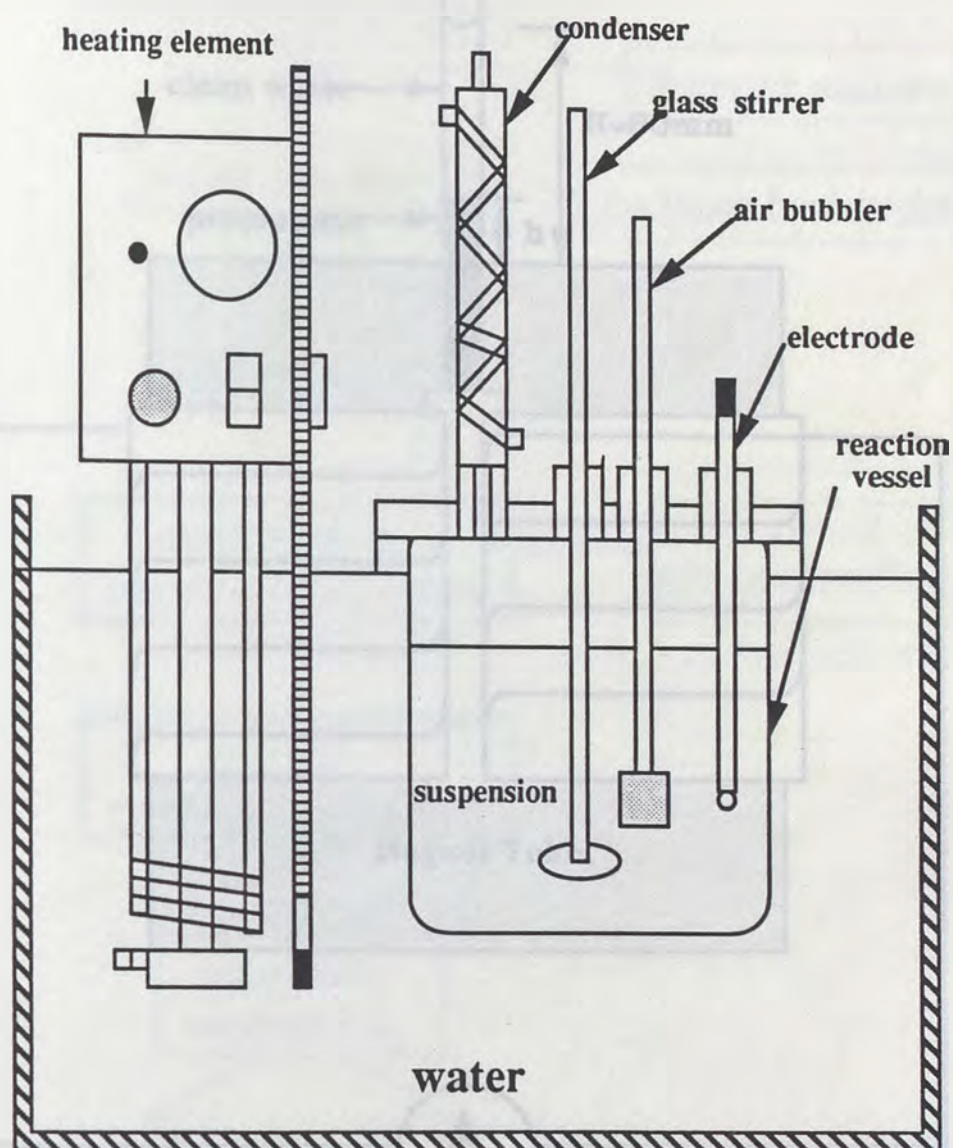


Figure 2.1. Schematic diagram of apparatus used in precipitation experiments at high temperature

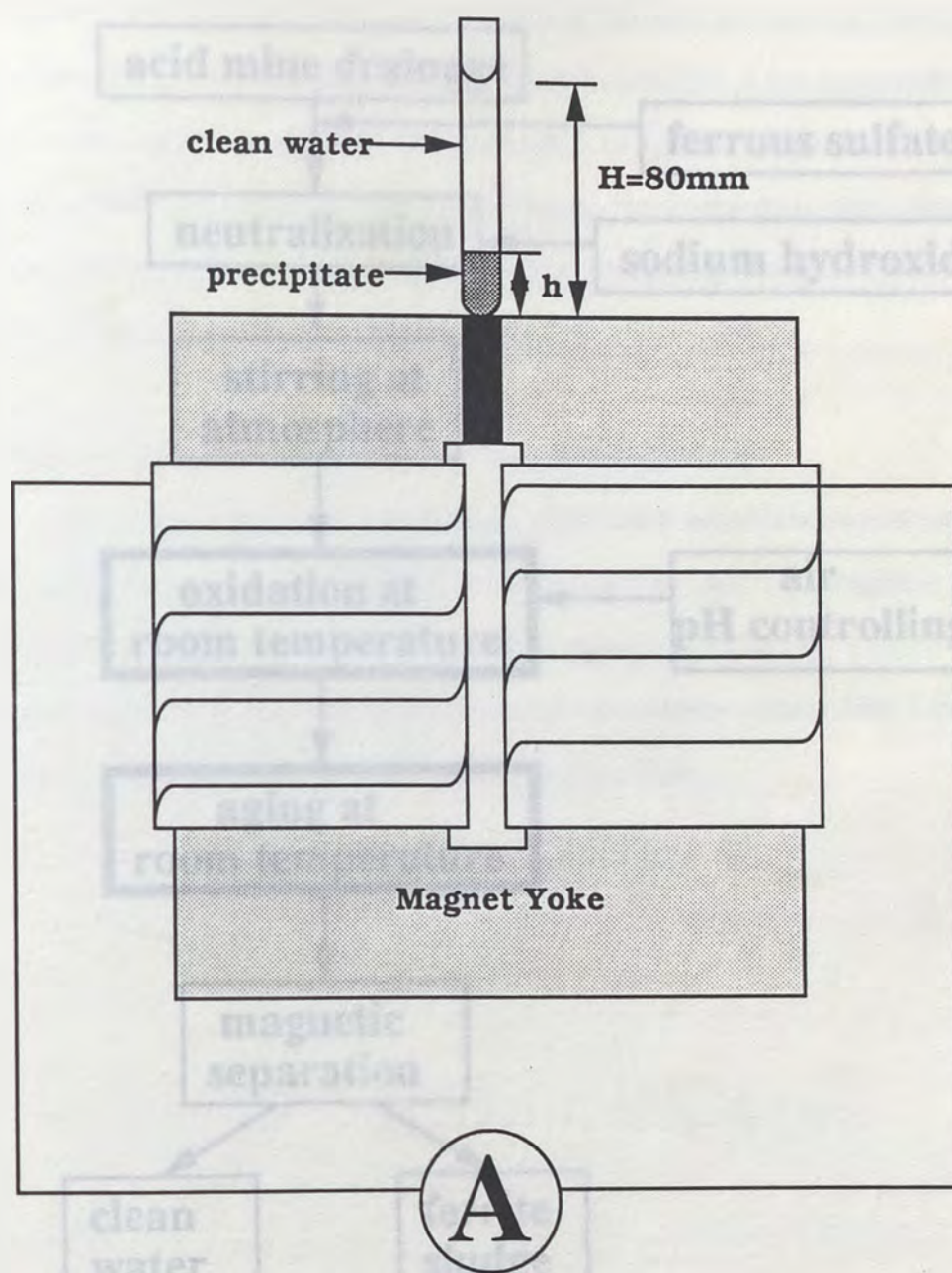


Figure 2.2. Schematic diagram of measuring settling height rate of precipitate at electrical magnetic field

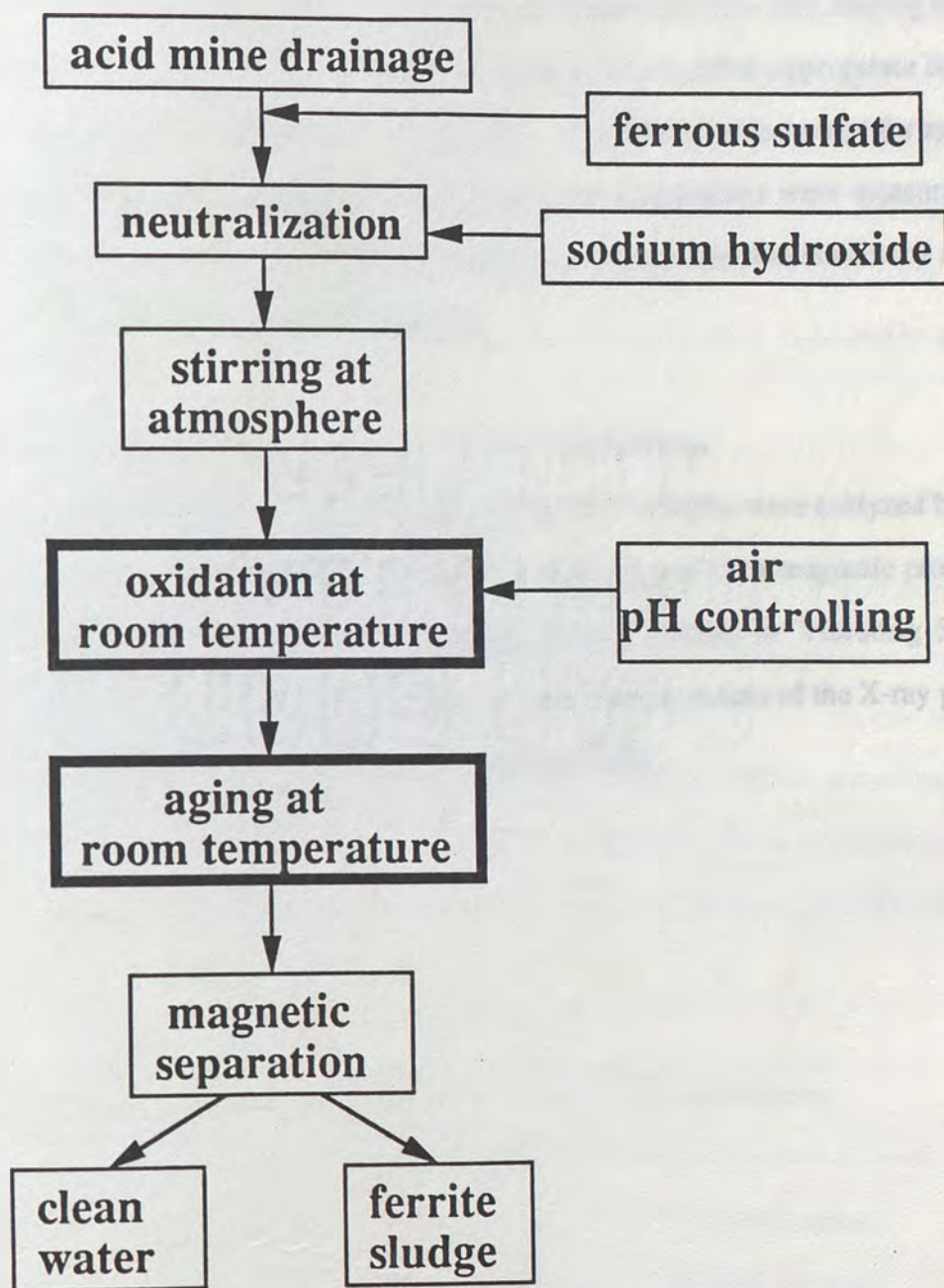


Figure 2.3. Experimental procedures of new modified ferrite precipitation at ambient temperature

suspension was green in color. Then the suspension was oxidized by sparged air through an air bubbler that was controlled by a flow meter at constant air flow rate. During stirring and oxidation, pH value was kept constant by adding NaOH. After appropriate time of oxidation, the measured suspension was taken into a 13 X 100mm culture tube for aging at ambient temperature. After required time of aging, the suspensions were measured the magnetic settling rate. The measurement of magnetic settling rate was conducted after 5 minutes at 1.5A applied electrical magnetic field.

2.4. Measurements of properties of ferrite precipitates

After magnetic separation or filtration, clean water samples were analyzed by ICP. Some precipitate samples were dried at room temperature, and their magnetic properties were measured by alternating Gradient Magnetometer (AGM) or Vibrating Sample Magnetometer (VSM). The dried precipitate was examined by means of the X-ray powder diffraction method using Cu-K α radiation and SEM or TEM.

3. Results and Discussions

In this investigation, both synthetic solutions and naturally occurring acid mine waters were used. Most of the initial experiments were conducted with synthetic solutions prepared with the addition of 20g $\text{FeSO}_4 \cdot 7\text{H}_2\text{O}/\text{l}$. The effect of different variables on synthetic solution were established. The information obtained from synthetic solutions were applied to actual water. In that regard results are divided into two distinct parts. Part I is related to the ferrite precipitated from synthetic solutions and Part II is related to the real acid mine waters.

3.1. Synthetic Solutions of $\text{FeSO}_4 \cdot 7\text{H}_2\text{O}$

The time of air oxidation is one of the most important factors to obtain the final ferrite precipitate. The effect of oxidation time with the ORP value of suspension, color and magnetic property of final precipitates after aging are given in Table 3.1. As can be seen, by increasing oxidation time the ORP changes slightly to abrupt. at the same time, color and magnetic properties also change. Color turns from green to brown through black. The magnetic property of black particles is strong as compared to brown particle which has weak magnetic property.

Table 3.1. Effect of Oxidation Time on ORP, Color and Magnetic Property

| Oxidation Time | -----> increase | | |
|-------------------|-------------------|-----------|-------------------|
| ORP | slightly increase | no change | abruptly increase |
| Color | green | black | brown |
| Magnetic Property | no | strong | weaker |

3.1.1. Effect of air oxidation time on oxidation-reduction potential (ORP)

Because the ORP value can be used to indicate different electrochemical equilibriums in suspension during oxidation, the abrupt ORP value change was often used to indicate that the reaction of ferrite formation had been completed during air oxidation at high temperature [23,42-44,48]. In this investigation, the ORP values of suspensions at different conditions were measured by the platinum combination electrode.

The effect of temperature of air oxidation The green suspensions were oxidized by sparging air at 0°C, 16°C, 40°C and 70°C. During the air oxidation, the pH value is kept in 10.5 by adding NaOH solution and the amount of air flow is 4266 s.c.cm/m.l.(standard cubic centimeter per minute per liter).

The relationship between ORP value of the suspension and air oxidation time at different temperature is shown in Figure 3.1.. By increasing oxidation temperature, the time taken to reach required ORP value for good magnetic particles can be decreased. As can be seen, 40-70°C, the abrupt change of ORP value can be accomplished is 10-12 minutes as compared to 20 minutes at low temperature. Several minutes later at lower temperature (comparing with Figure 3.4.) is because several minutes are needed to reach thermal equilibrium as indicated in Instructions of Fisher pH meter [57].

There are several reactions during oxidation of ferrous hydroxide [52, 58-63]. Although some reactions and intermediates are still not clear, in general the half-cell reaction equation can be written as:



where A_s is iron oxide, hydroxide, oxyhydroxide or their mixture with higher average valence and B_s is iron oxide, hydroxide, oxyhydroxide or their mixture with lower average valence. According to Nernst's equation, one has

$$E = E^\circ - 2.3 RT/F \cdot (m/n) \text{ pH} \quad (3-2)$$

From equation (3-2), one can know that increase of temperature decrease the ORP value of suspension is shown in Figure 3.1.

The effect of pH value The deep green suspensions were oxidized at different pH values at same temperature. The pH value of suspension were controlled at 9.5, 10.5, 11.5 and 12.5 by adding NaOH solution. The other experimental procedures, methods and conditions were same as above.

The relationship between ORP values of the suspension and air oxidation time at different pH values in Figure 3.2, is similar to Figure 3.1. The time taken to reach required ORP value for good magnetic particles is 15 minutes. The abrupt ORP change is consistent with the change from strong magnetic to weak magnetic precipitate except at pH 9.5. Comparing with Figure 3.1, however the intermediate oxidation reactions are different. The decrease in ORP value decrease with increase in pH value can be explained by the equation (3.2).

The effect of amount of air flow The deep green suspensions were oxidized by different amount of air flow. The amounts of air flow were controlled at 1, 2, 4 and 8 L/min. The other experimental procedures, methods and conditions were same as above. The relationship between ORP value of the suspension and air oxidation time at different air flow amounts in Figure 3.3, is similar to Figure 3.1. By increasing the amount of air flow, the time taken to reach required ORP value for good magnetic particles can be decreased. As can be seen, if air flow is larger than 4 L/min, i.e. twice, the abrupt change of ORP value can be accelerated at 5-15 minutes as compared to 50 minutes at low air flow. It means large (comparing with Figure 3.6.) at 1783 s.c.c.m./min. It means there was almost no stirring effect in the suspension. That the trend

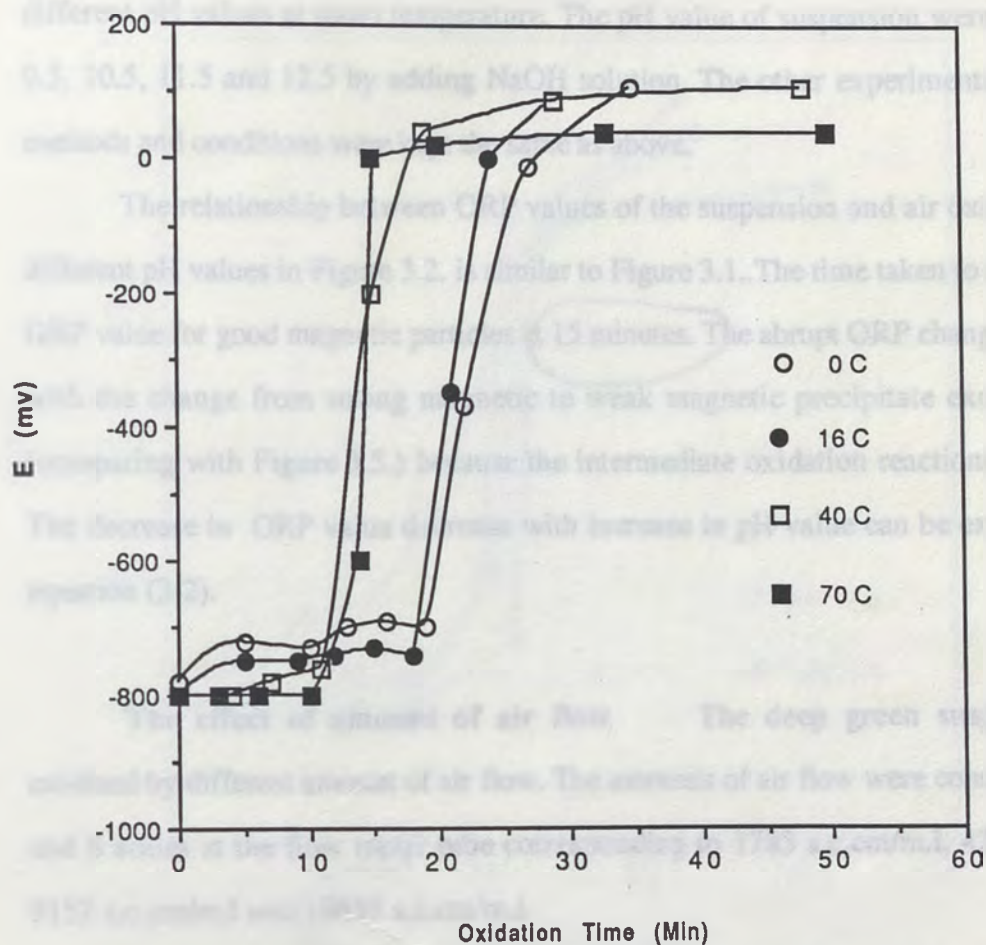


Figure 3.1. Relationship between ORP value of the suspension and oxidation time at different temperature

From equation (3-2), one can know that increase of temperature decrease the ORP value of suspension as shown in Figure 3.1.

The effect of pH value The deep green suspensions were oxidized at different pH values at room temperature. The pH value of suspension were controlled at 9.5, 10.5, 11.5 and 12.5 by adding NaOH solution. The other experimental procedures, methods and conditions were kept the same as above.

The relationship between ORP values of the suspension and air oxidation time at different pH values in Figure 3.2. is similar to Figure 3.1..The time taken to reach required ORP value for good magnetic particles is 15 minutes. The abrupt ORP change is consistent with the change from strong magnetic to weak magnetic precipitate except at pH 9.5 (comparing with Figure 3.5.) because the intermediate oxidation reactions are different. The decrease in ORP value decrease with increase in pH value can be explained by the equation (3-2).

The effect of amount of air flow The deep green suspensions were oxidized by different amount of air flow. The amounts of air flow were controlled at 1, 2, 4 and 8 scales at the flow meter tube corresponding to 1783 s.c.cm/m.l, 4266 s.c.cm/m.l, 9152 s.c.cm/m.l and 19649 s.c.cm/m.l.

The relationship between ORP value of the suspension and air oxidation time at different amount of air flow shown in Figure 3.3. is similar to these in Figure 3.1. and 3.2.. By increasing air flow, the time taken to reach required ORP value for good magnetic particles can be decreased. As can be seen, if fair flow is larger than 4266 s. c. cm/m.l., the abrupt change of ORP value can be accomplished is 8-15 minutes as compared to 50 minutes at low air flow. 11 minute longer (comparing with Figure 3.6.) at 1783 s.c.cm/m.l. is because there was almost no stirring effect in the suspension. That the trend

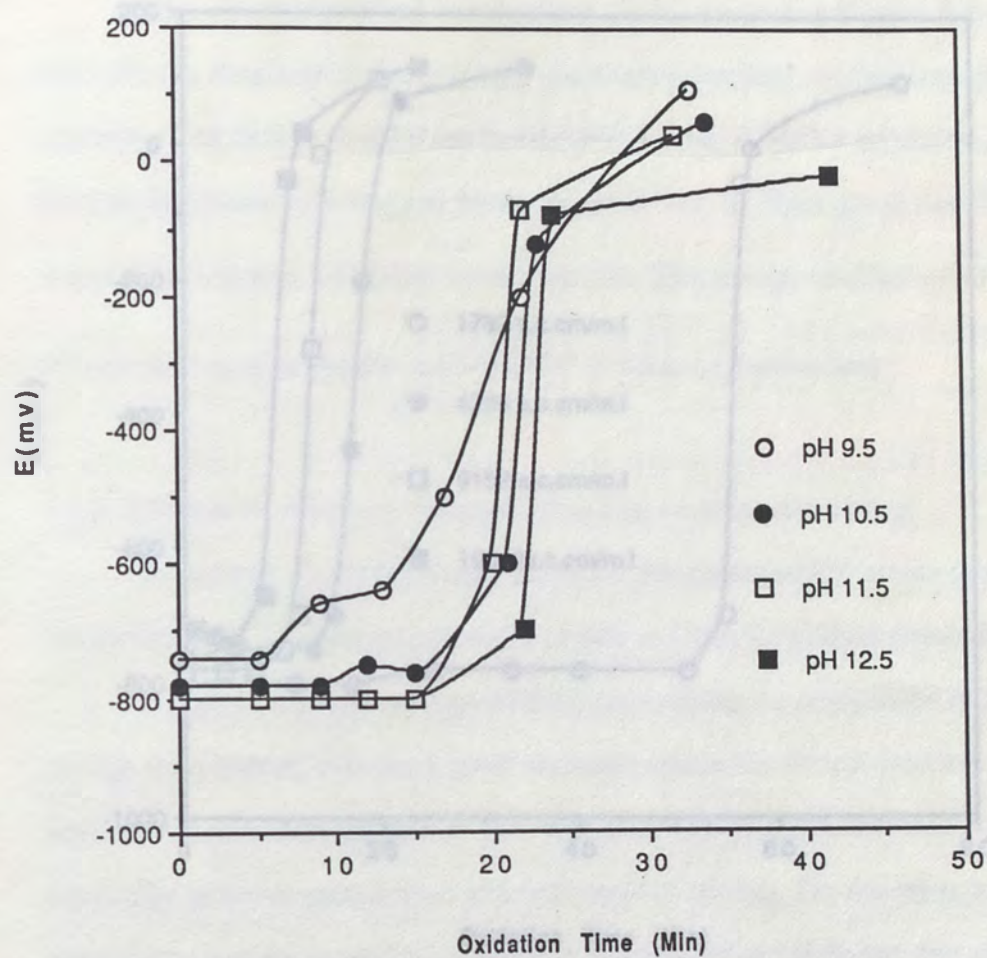


Figure 3.2. Relationship between ORP value of the suspension and oxidation time at different pH value

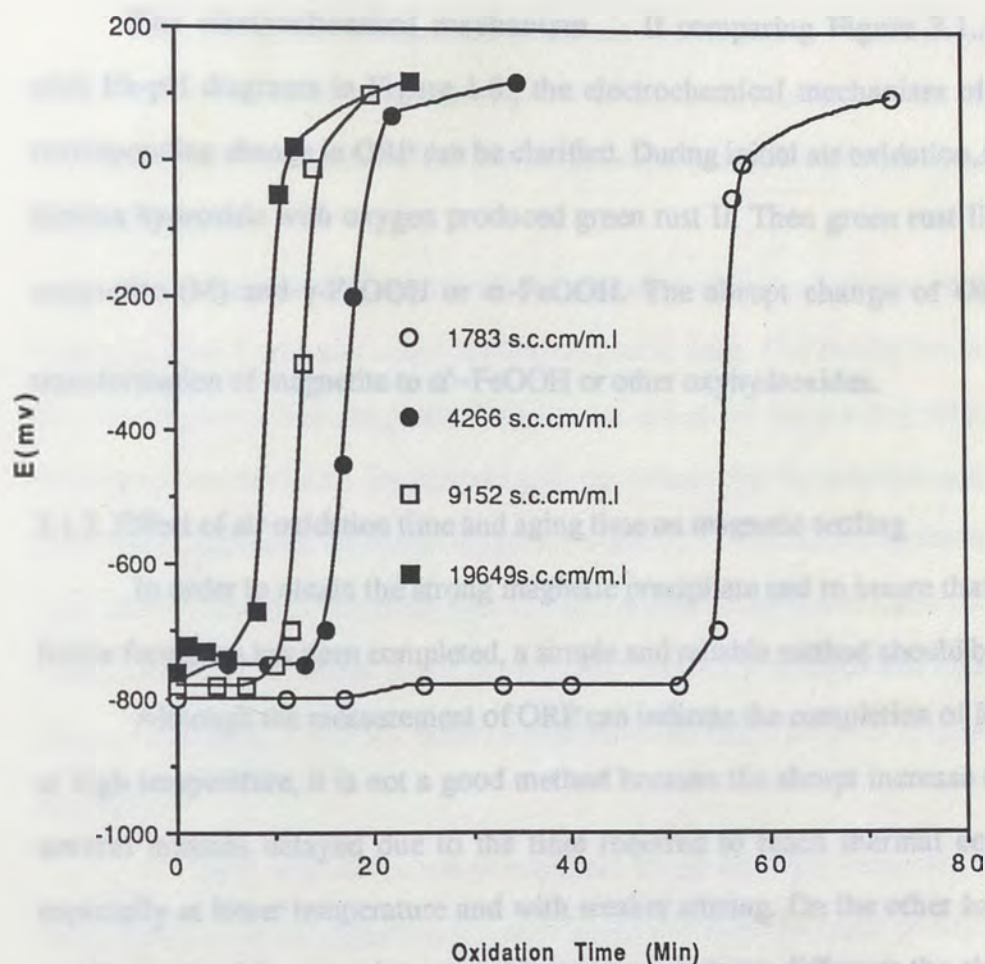


Figure 3.3. Relationship between ORP value of the suspension and oxidation time at different amount of air flow

of ORP value which increases with increase in air flow is attributed to the fact that pH value of suspension near the electrode is decreased by the added air and that the added OH^- ion can not immediately migrate to the electrode.

The electrochemical mechanism If comparing Figure 3.1., 3.2. and 3.3. with Eh-pH diagrams in Figure 1.8., the electrochemical mechanism of reactions and corresponding change in ORP can be clarified. During initial air oxidation, the reaction of ferrous hydroxide with oxygen produced green rust II. Then green rust II is oxidized to magnetite (M) and $\gamma\text{-FeOOH}$ or $\alpha\text{-FeOOH}$. The abrupt change of ORP reflects the transformation of magnetite to $\alpha'\text{-FeOOH}$ or other oxyhydroxides.

3.1.2. Effect of air oxidation time and aging time on magnetic settling

In order to obtain the strong magnetic precipitate and to insure that the reaction of ferrite formation has been completed, a simple and reliable method should be developed.

Although the measurement of ORP can indicate the completion of ferrite formation at high temperature, it is not a good method because the abrupt increase of ORP may be several minutes delayed due to the time required to reach thermal equilibrium [57], especially at lower temperature and with weaker stirring. On the other hand the reaction mechanism and the procedure at ambient temperature are different; the abrupt increase in ORP does not completely correspond to the formation of ferrite, as the complete ferrite formation occurs after air oxidation and aging.

The measurement of magnetization curve (B-H curve) is a good method to measure magnetic properties of dried final precipitate, but it can not directly measure the magnetic properties of the precipitate in suspension.

In this investigation, the magnetic settling rates of precipitate at different conditions

were measured as a function of air oxidation time and aging time. To measure the ratio of height h/H of precipitates in suspensions can qualitatively compare the magnetic properties of precipitates in suspension and obtain the optimum condition.

The effect of temperature on air oxidation The magnetic rate of precipitate was measured by removing 8ml of suspension in a 13 X 100 mm culture tube intermittently. The suspensions in the culture tubes were all aged for an extended time at ambient condition.

The magnetic settling rates of precipitates obtained at different oxidation time were measured after 5 minutes under applied magnetic field. The results are shown in Figure 3.4. which shows that magnetic field has no effect on the settling rate of precipitates without any air oxidation. By increasing air oxidation time the magnetic settling rates of the precipitates increased. However, longer air oxidation is detrimental to the magnetic settling rate. The critical time increases with the decrease of temperature. The strongly magnetic precipitates can be settled down by magnetic field in 5 minutes and show the magnetic property of Fe_3O_4 . Table 3.2. shows the effect of oxidation time on magnetic properties of the sludge.

At 70°C and 40°C , the precipitates show strongly magnetic property almost immediately after air oxidation which is consistent with the result of Kiyama [47], but at 16°C and 0°C , the precipitates show strong magnetic property only after aging several hours at room temperature.

The results show the strongly magnetic precipitate Fe_3O_4 can be obtained by air oxidation at room temperature even at 0°C provided longer oxidation and aging time are given. However, by increasing temperature, oxidation and aging time can be reduced. One of objectives of the investigation is to precipitate ferrite at room temperature.

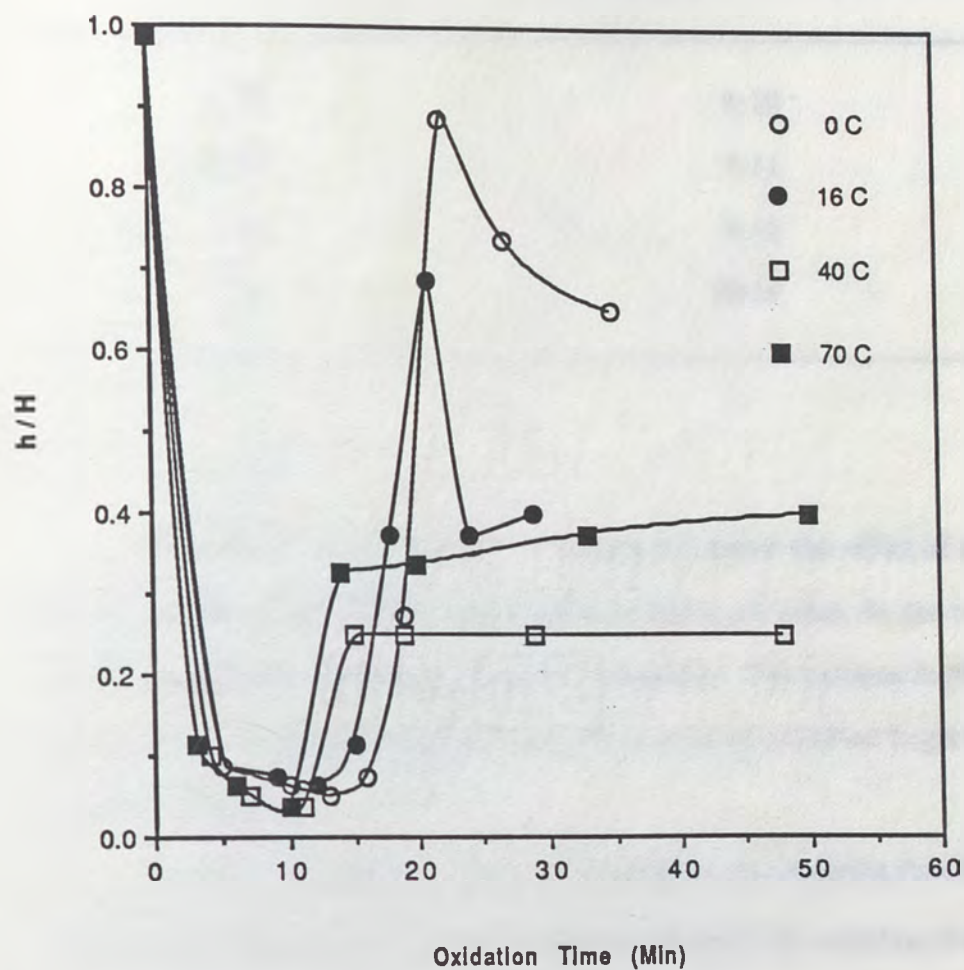


Figure 3.4. Effect of oxidation time on settling height ratio of precipitates obtained at different temperature

Table 3.2. Temperature and Oxidation Time to Obtain Strongly Magnetic Precipitate

| Temperature (°C) | Oxidation Time for Strong magnetic Precipitate (Minutes) |
|------------------|---|
| 70 | 6-10 |
| 40 | 7-11 |
| 16 | 9-12 |
| 0 | 10-16 |

The effect of pH value Figure 3.5 shows the effect of oxidation time on settling height of the precipitate obtained at different pH value. As can be seen, above pH 10.5, the precipitate shows good magnetic properties. The increase in pH value increases the time range of oxidation and decreases the time of air oxidation to get the final, strongly magnetic precipitates.

Although the higher pH value is advantageous to obtaining final ferrite precipitate, reagent consumption and constraint on effluent pH led to the selection of an optimum pH of 10.5 in all other experiments.

The effect of amount of air flow Figure 3.6. shows the effect of oxidation time on settling height of the precipitate obtained at different air flow. As can be seen, the increase of air flow increases the time range of oxidation and decreases the time of air oxidation to get the final, strongly magnetic precipitates.

Although the increase in the amount of air flow is advantageous to obtaining final

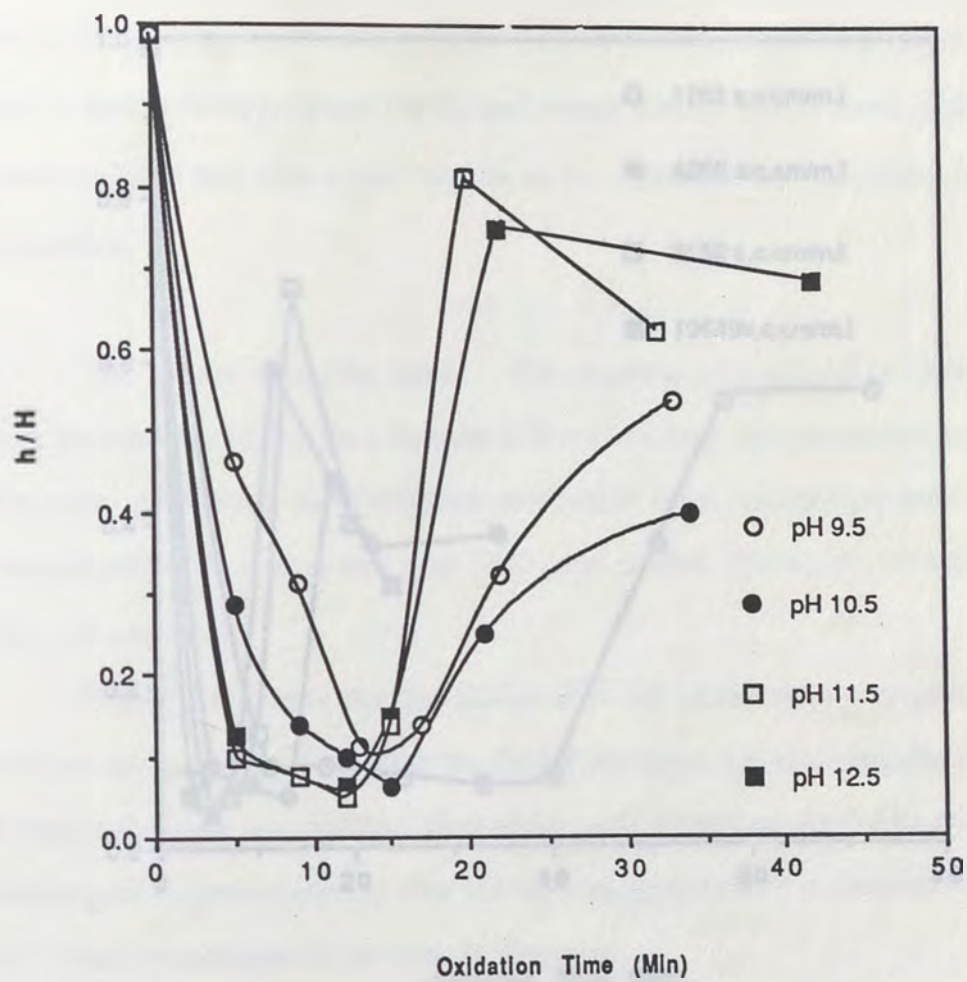


Figure 3.5. Effect of oxidation time on settling height ratio of precipitates obtained at different pH value

ferite, the amount of air flow was controlled at about 4266 s.c.cm/m.l in all other experiments in order to conduct experiments easily.

The effect of Fe_2O_3 seed

The deep green suspension with and without

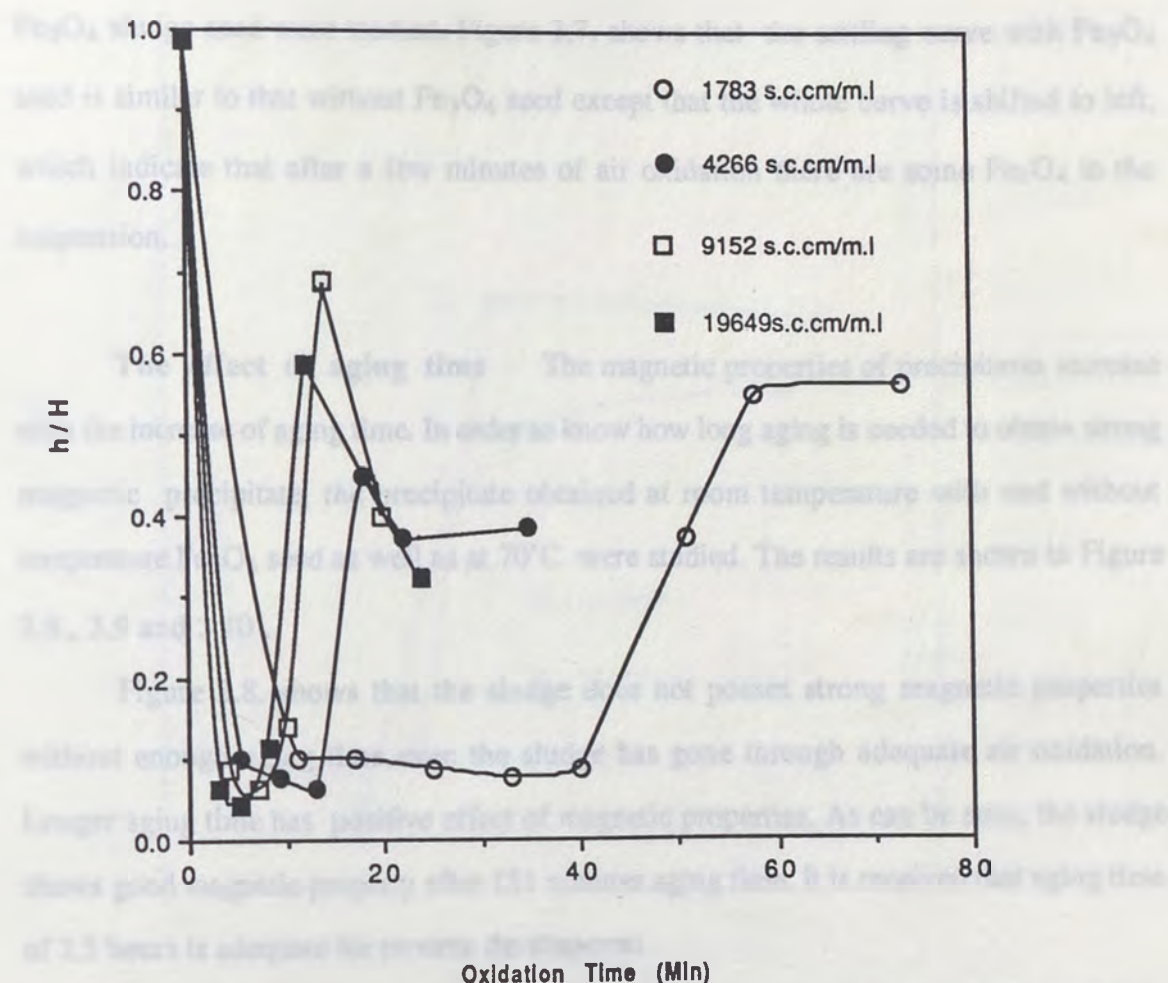


Figure 3.6. Effect of oxidation time on settling height ratio of precipitates obtained at different amount of air flow

ferrite, the amount of air flow was controlled at about 4266 s.c.cm/m.l in all other experiments in order to control experiments easily.

The effect of Fe_3O_4 seed The deep green suspension with and without Fe_3O_4 sludge seed were studied. Figure 3.7. shows that the settling curve with Fe_3O_4 seed is similar to that without Fe_3O_4 seed except that the whole curve is shifted to left, which indicate that after a few minutes of air oxidation there are some Fe_3O_4 in the suspension.

The effect of aging time The magnetic properties of precipitates increase with the increase of aging time. In order to know how long aging is needed to obtain strong magnetic precipitate, the precipitate obtained at room temperature with and without temperature Fe_3O_4 seed as well as at 70°C were studied. The results are shown in Figure 3.8., 3.9 and 3.10 .

Figure 3.8. shows that the sludge does not posses strong magnetic properties without enough aging time even the sludge has gone through adequate air oxidation. Longer aging time has positive effect of magnetic properties. As can be seen, the sludge shows good magnetic property after 151 minutes aging time. It is received that aging time of 2.5 hours is adequate for process development .

Figure 3.9 shows the effect of aging time on the settling height ratio of precipitate with additional Fe_3O_4 seeding material. The precipitate shows strong magnetic property even only 5 minute aging because of adding Fe_3O_4 seed to the precipitate. The precipitate can be settled down very quickly in magnetic field after aging of 117 minutes.

Figure 3. 10. shows the effect of aging time on the ferrite precipitate prepared at 70°C . As can be seen, to get strong magnetic sludge after high temperature oxidation need significantly less aging time as compared to after room temperature oxidation.

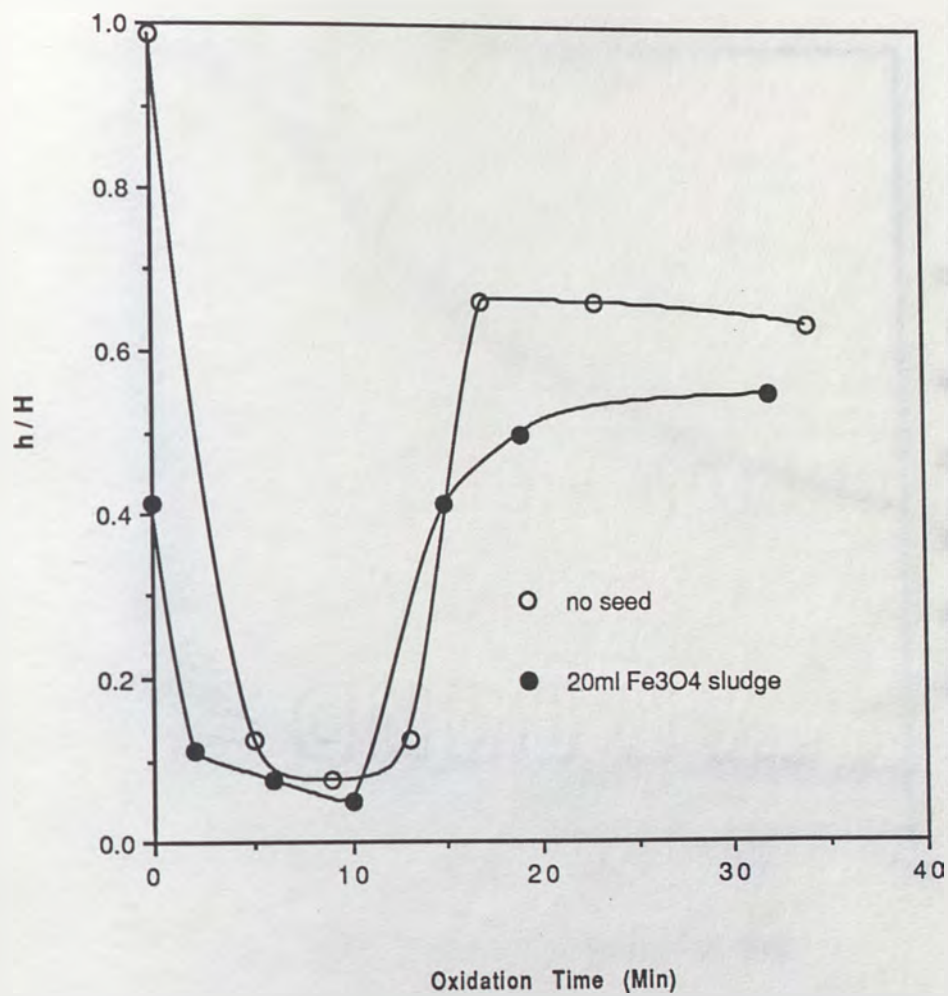


Figure 3.7. Effect of oxidation time on settling height ratio of precipitates obtained with or without Fe₃O₄ seed

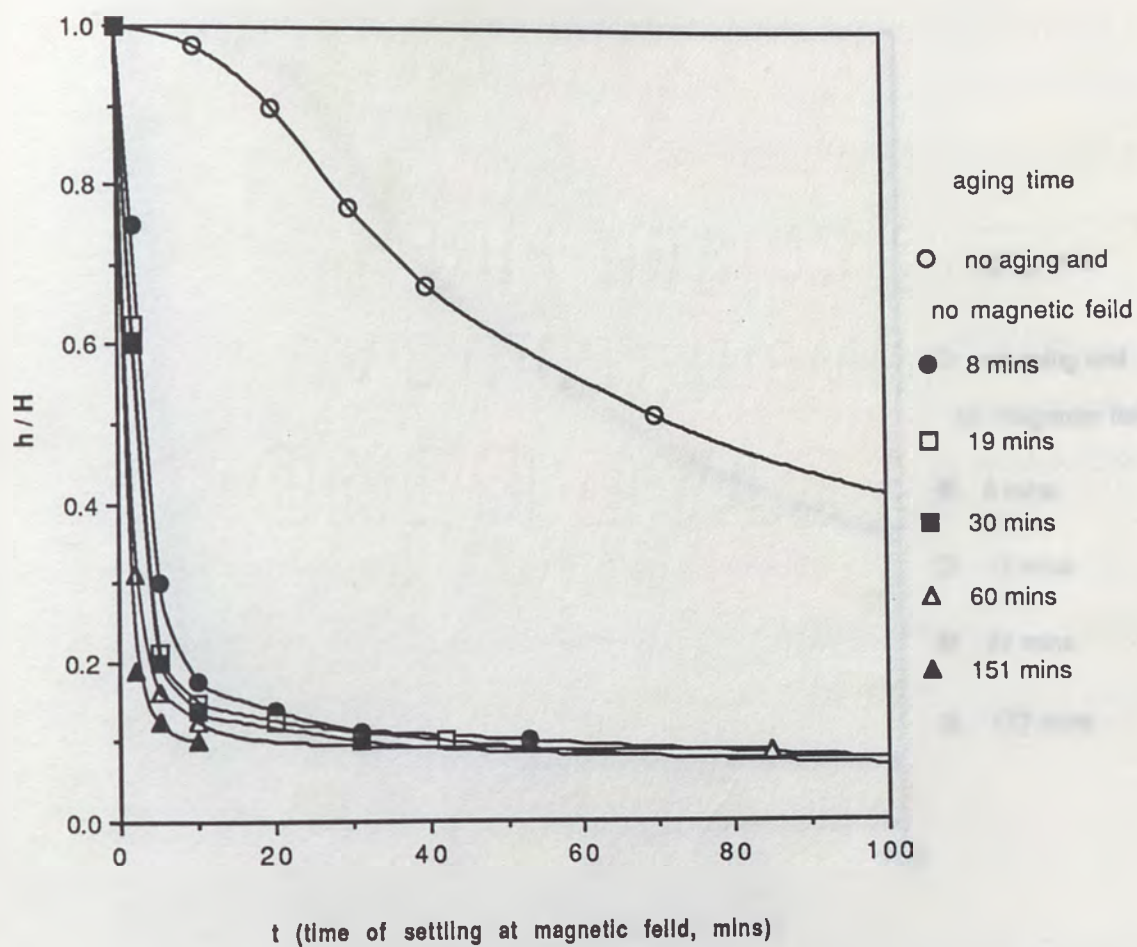


Figure 3.8. Effect of aging time on the settling height ratio of precipitate obtained at room temperature

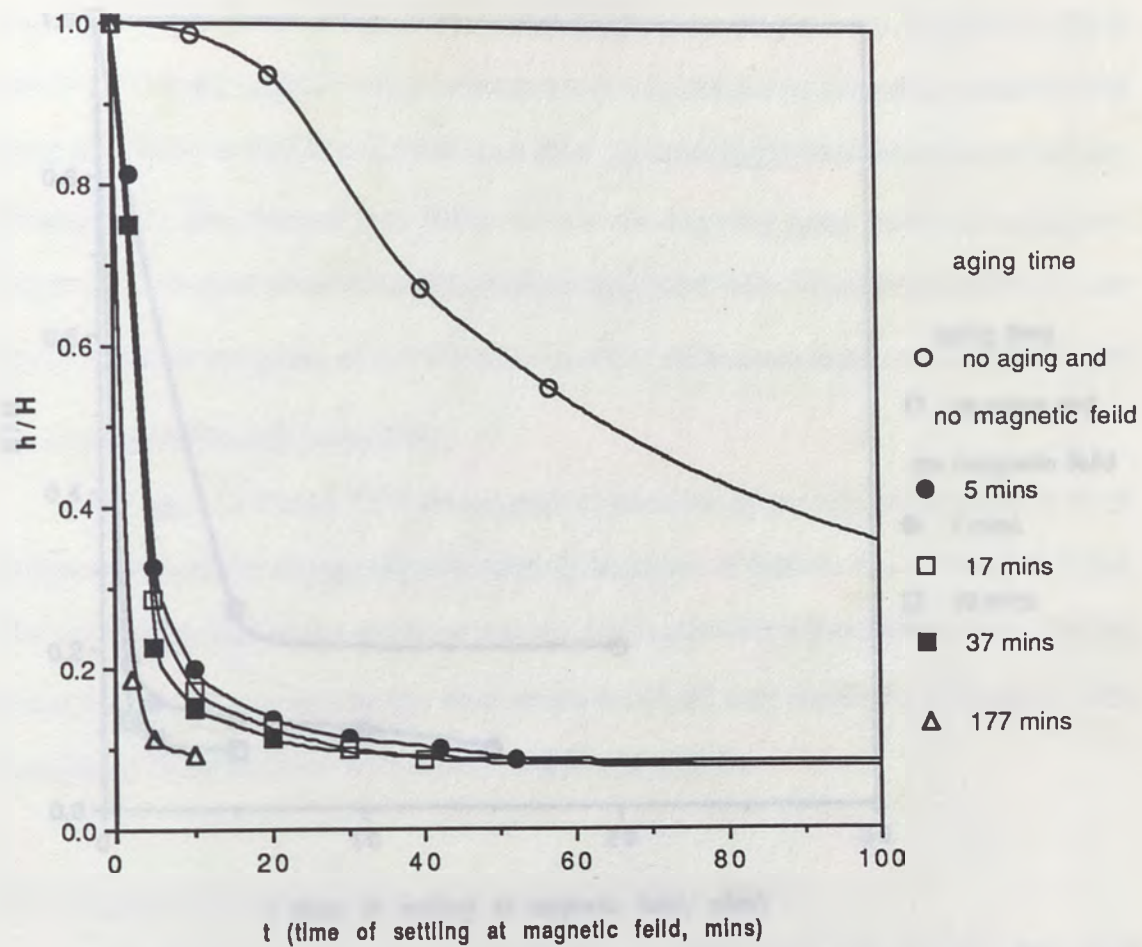


Figure 3.9. Effect of aging time on the settling height ratio of precipitate obtained at room temperature with Fe_3O_4 seed

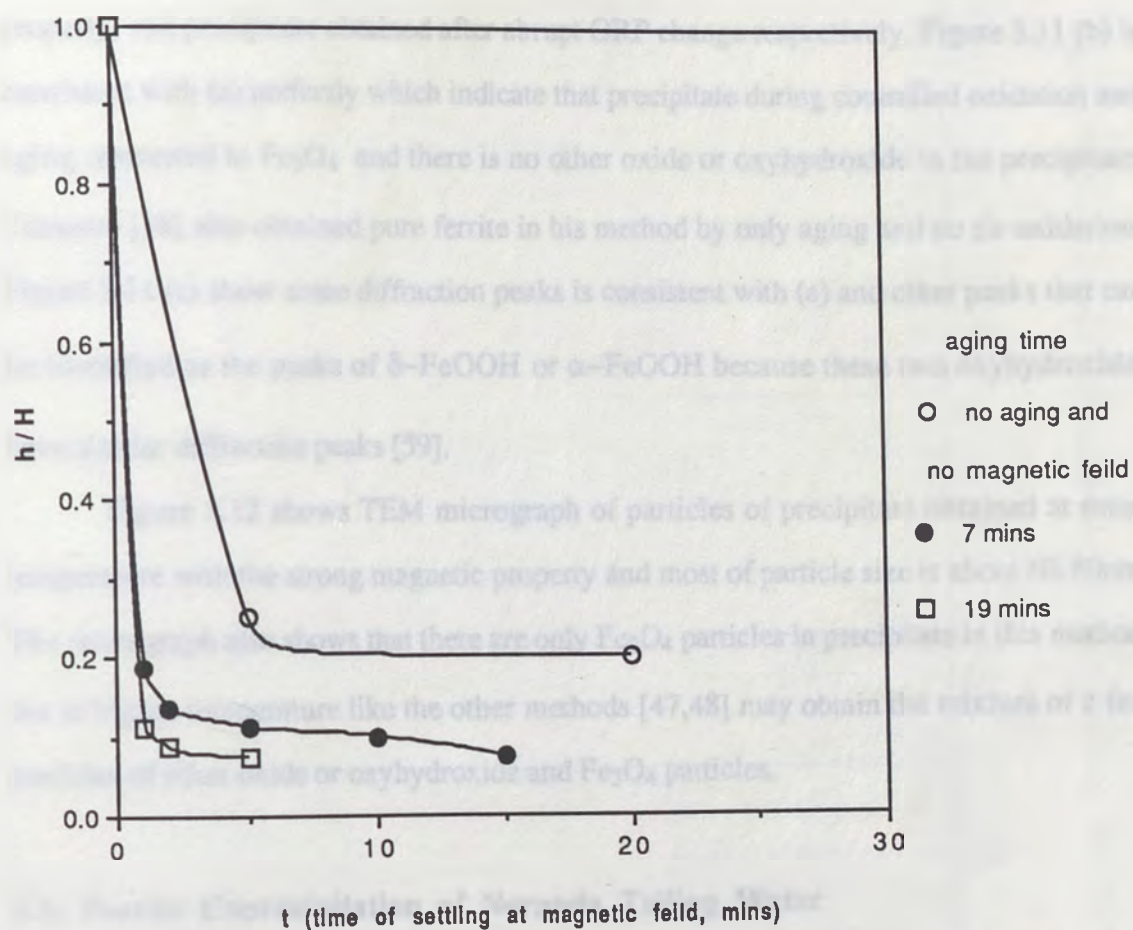


Figure 3.10. Effect of aging time on the settling height ratio of precipitate obtained at 70°C

3.1.3. The characteristics of precipitates

Figure 3.11 (a), (b) and (c) show the standard X-ray powder diffraction powder of Fe_3O_4 , magnetic precipitate obtained at room temperature with the strongest magnetic property, and precipitate obtained after abrupt ORP change respectively. Figure 3.11 (b) is consistent with (a) perfectly which indicate that precipitate during controlled oxidation and aging converted to Fe_3O_4 and there is no other oxide or oxyhydroxide in the precipitate. Tamaura [38] also obtained pure ferrite in his method by only aging and no air oxidation. Figure 3.11 (c) show some diffraction peaks is consistent with (a) and other peaks that can be identified as the peaks of $\delta\text{-FeOOH}$ or $\alpha\text{-FeOOH}$ because these two oxyhydroxides have similar diffraction peaks [59].

Figure 3.12 shows TEM micrograph of particles of precipitate obtained at room temperature with the strong magnetic property and most of particle size is about 60-80nm. The micrograph also shows that there are only Fe_3O_4 particles in precipitate in this method, but at higher temperature like the other methods [47,48] may obtain the mixture of a few particles of other oxide or oxyhydroxide and Fe_3O_4 particles.

3.2. Ferrite Coprecipitation of Noranda Tailing Water

Noranda Tailing Water contains a high concentration of Zn, Fe, Mg, Ca, Mn, small amount of Al, Pb and Cd (Table 3.3.) with pH 3.5. Since the Fe/M molar ratio, where M is other metal ions (II, III), is an important factor to coprecipitate ferrite [43,44], it was decided to study the coprecipitation at room temperature as a function of Fe/M molar ratio and time. As established earlier, the amount of air flow was kept at about 4266 s.c.cm./m.l., and pH value was maintained at about 10.5.

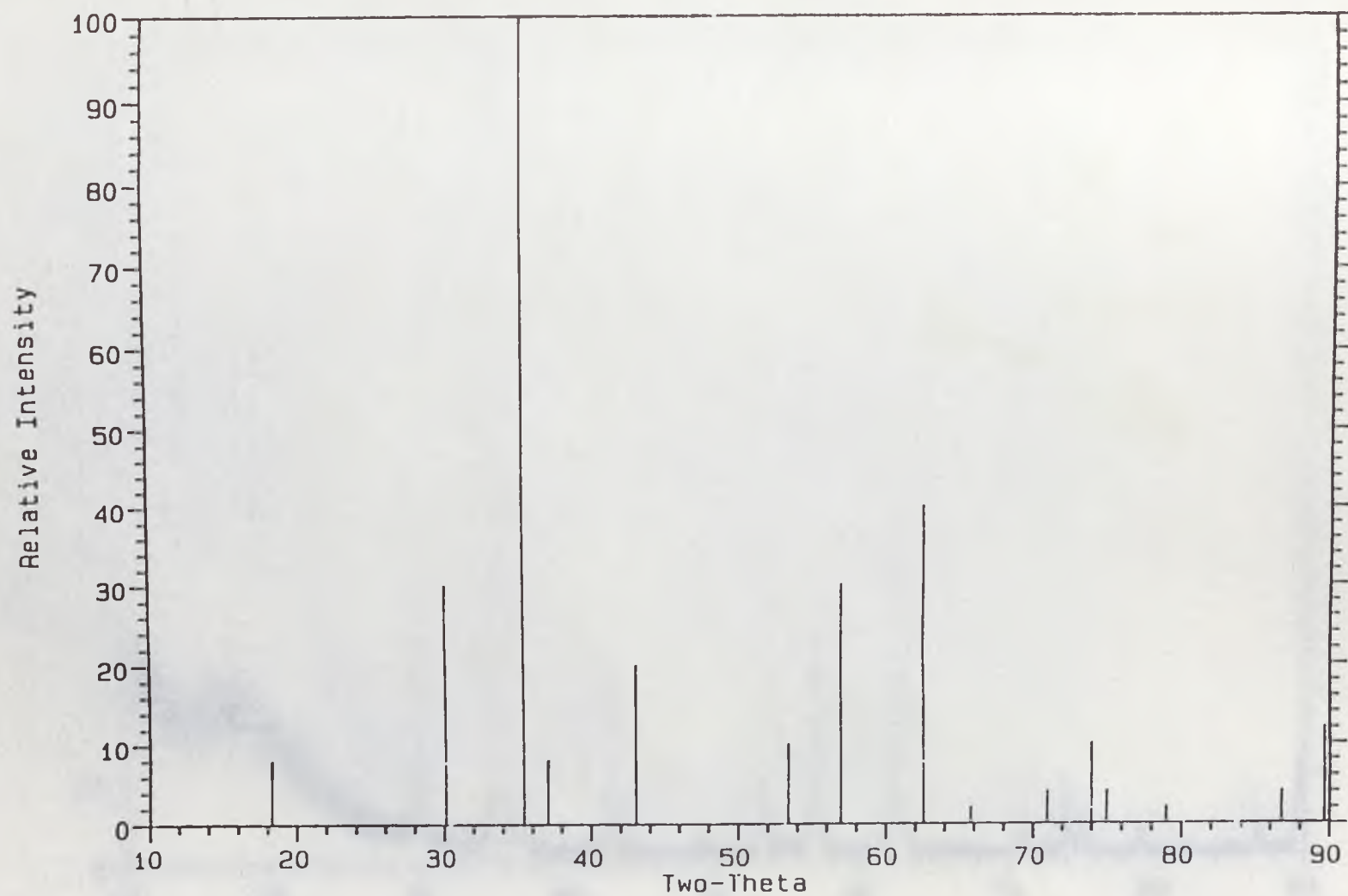


Figure 3.11 (a). Standard X-ray powder diffraction pattern of Fe₃O₄, Cu-Kα

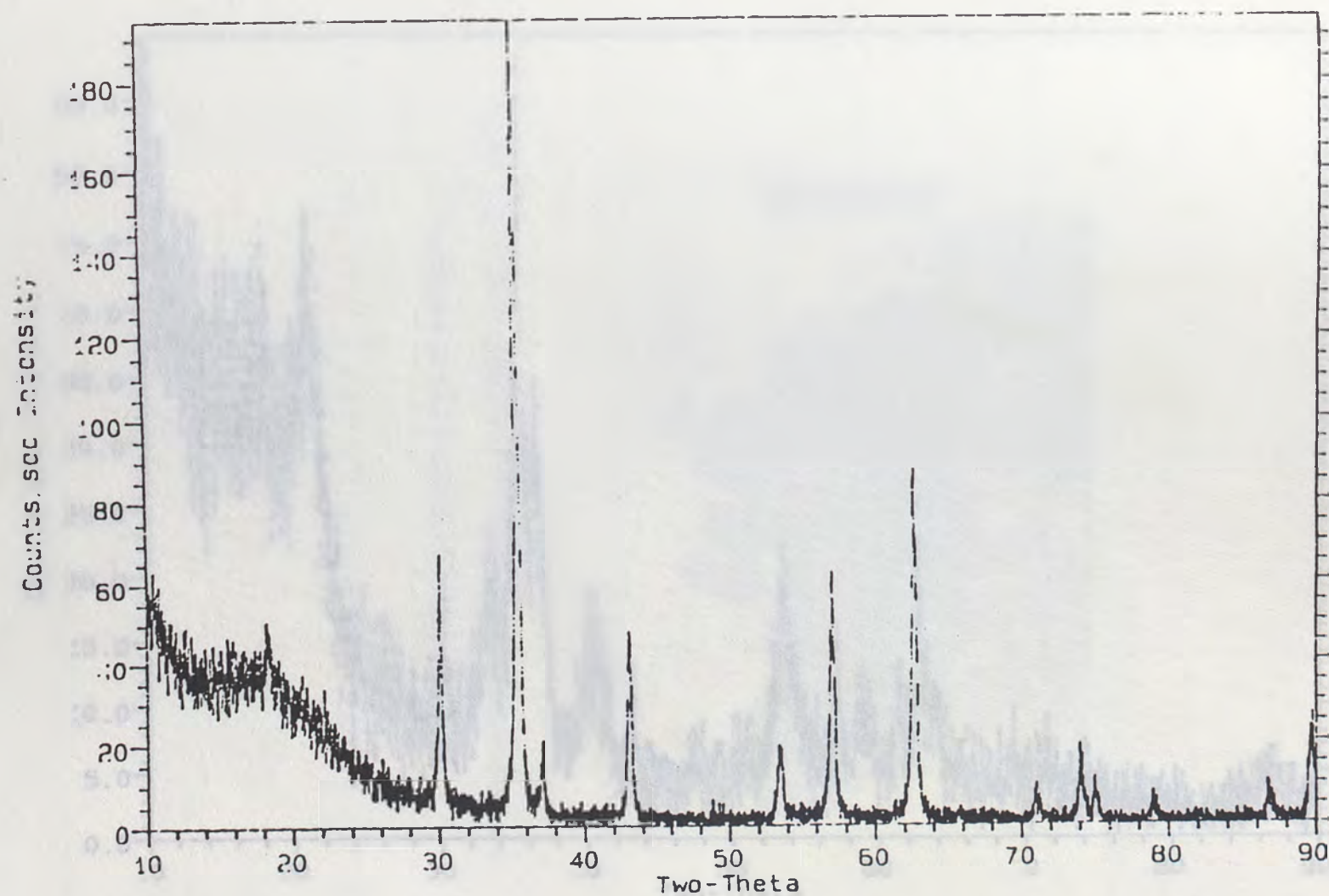


Figure 3.11 (b). X-ray powder diffraction of precipitate obtained at room temperature with the strongest magnetic property, Cu-K α

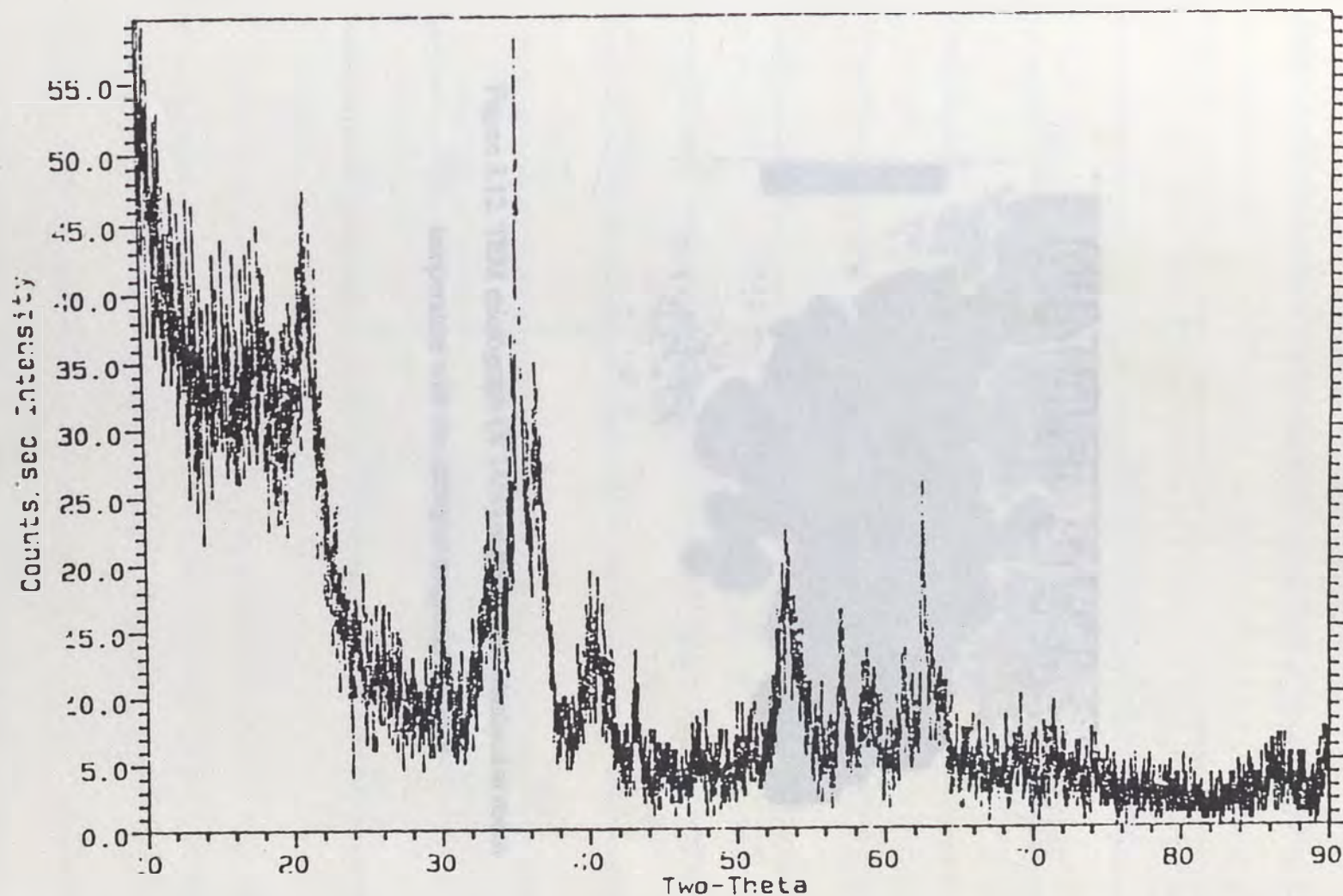


Figure 3.11 (c). X-ray powder diffraction of precipitate obtained at room temperature after ORP abrupt change, Cu-K α

Table 3.3. Characterization of heavy metals in Florida Tailing Sludge and treated water

| Concentration of Heavy Metals (mg/kg) | | |
|---------------------------------------|--------|---------------|
| Element | Sludge | Treated water |
| Pb | 15.2 | 0.1 |
| Cd | 0.8 | 0.1 |
| Fe | 3.2 | 0.1 |
| Mn | 21.2 | 21.2 |
| Cu | 154.9 | 145.0 |

Figure 3.12. TEM micrograph (X 145k) of precipitate obtained at room temperature with the strongest magnetic property

3.2.1. The settling rate of precipitates from Noranda Tailing Water

Figure 3.13 shows that effect of air saturation time on settling height ratio of

Table 3.3. Concentrations of heavy metals in Noranda Tailing Water and treated water

| Elements | Concentration of heavy metals(ppm) | |
|----------|------------------------------------|---------------|
| | Noranda Tailing Water | Treated water |
| Fe | 286.2 | <0.1 |
| Zn | 125.5 | 0.1 |
| Mn | 79.9 | 0.1 |
| Al | 13.2 | <0.1 |
| Cd | 0.4 | <0.1 |
| Pb | 3.2 | 0.1 |
| Mg | 226.7 | 25.8 |
| Ca | 354.9 | 345.0 |

3.2.1. The settling rate of precipitates from Noranda Tailing Water

Figure 3.13 shows that effect of air oxidation time on settling height ratio of precipitates obtained at room temperature from Noranda Tailing Water as a function of Fe/M molar ratio of 0, 1, 3 and 5. Without the addition of FeSO_4 , the precipitates did not show any magnetic properties even for an extended oxidation time. An increase in Fe/M molar ratio increased magnetic property and an optimum magnetic property was noticed at about 20 minutes oxidation time. In one experiment, aging time was increased from 27 hours to 49 hrs. As can be seen, increasing aging time increased magnetic property (as determined by magnetic settling rates).

The magnetic properties of dried precipitates were measured by Alternating Gradient Magnetometer (AGM) as shown in Figure 3.14.. The precipitates obtained from Noranda Tailing Water with Fe/M molar ratio of 5 were respectively oxidized 10 and 20 minutes, then aged 2 days and dried. The saturation magnetization of the precipitate oxidized 10 minutes is only 37.9 emu/g, and that of the precipitate oxidized 20 minutes is 60 emu/g. This is consistent with the results of magnetic settling rate.

3.2.2. The results of treated Noranda Tailing Water and characteristics of the precipitate

Noranda Tailing Water was treated by the modified ferrite precipitation with Fe/M molar ratio of 5. Table 3.3. indicates that the metal ions were completely removed by modified ferrite precipitation except for Mg and Ca ions which are not concerned by various industrial standards at the present time.

The characteristics of the precipitate obtained are measured. The X-ray diffraction pattern of the precipitate is shown in Figure 3.15. By comparing with standard diffraction pattern of Fe_3O_4 in Figure 3.11(a), it can be observed that the precipitate has the identical pattern of Fe_3O_4 , a spinel ferrite. In the pattern of the precipitate, a slight shift of 2θ angles and difference in intensity of diffraction peaks is observed. This is due to some

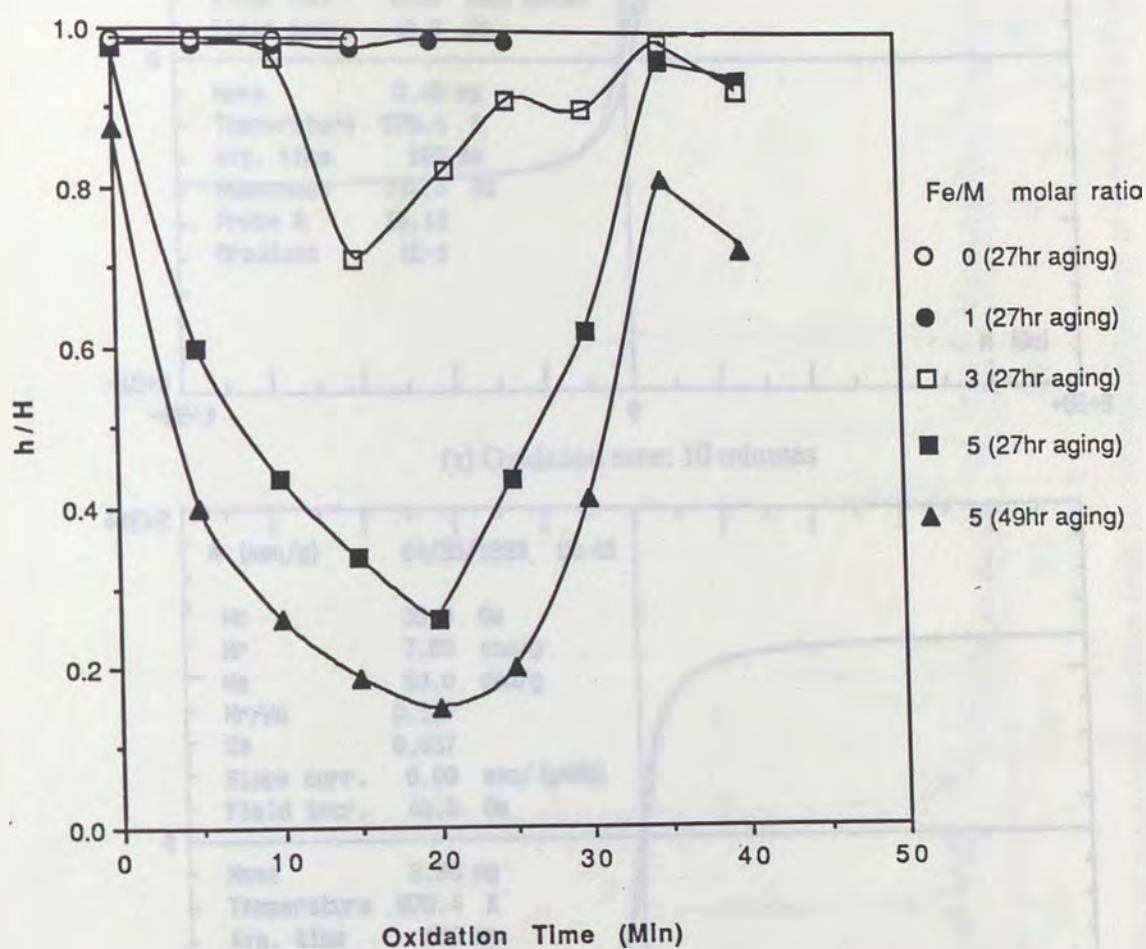
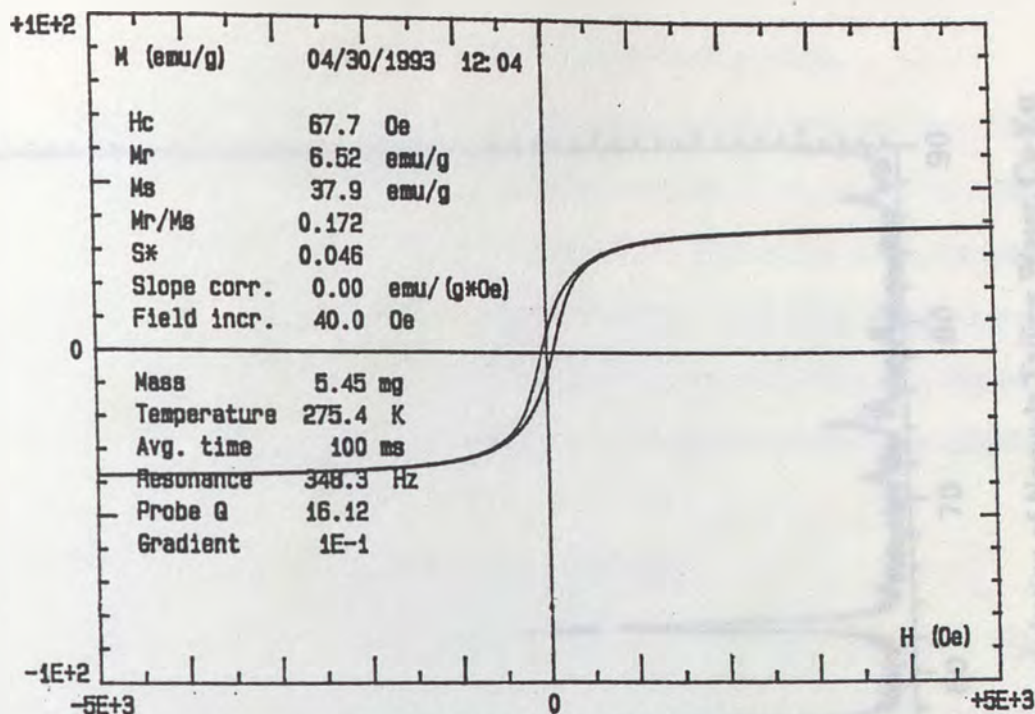
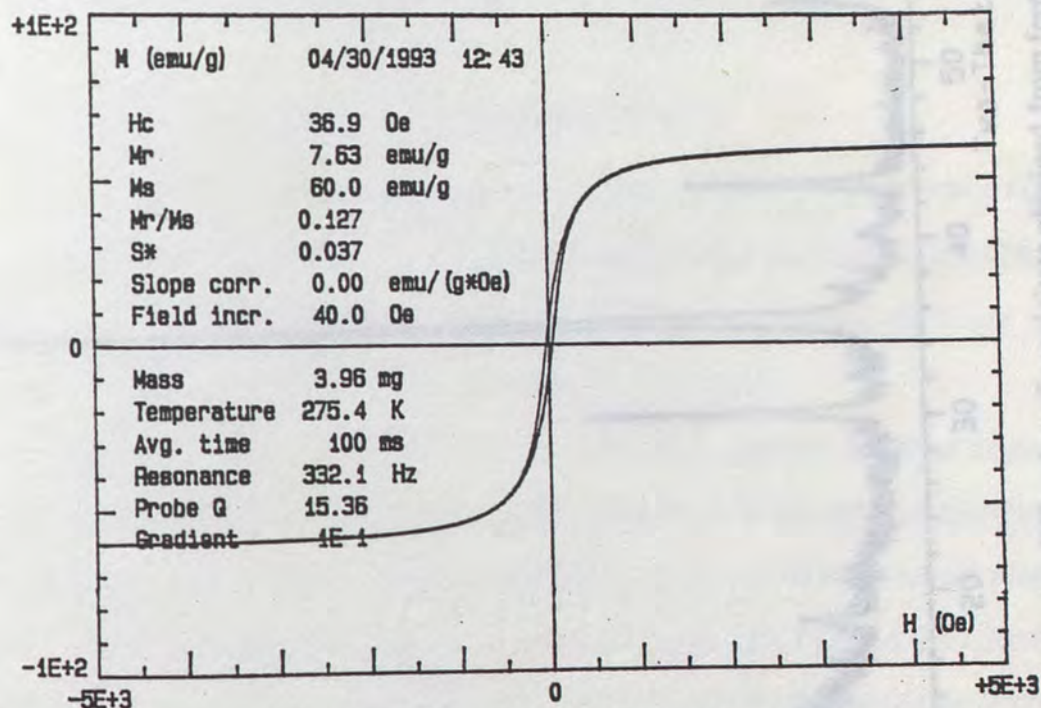


Figure 3.13. Effect of oxidation time on settling height ratio
of precipitates obtained from Noranda Tailing Water



(a) Oxidation time: 10 minutes



(b) Oxidation time: 20 minutes

Figure 3.14. Magnetization curve of precipitate obtained from ferrite coprecipitation of Noranda Tailing Water

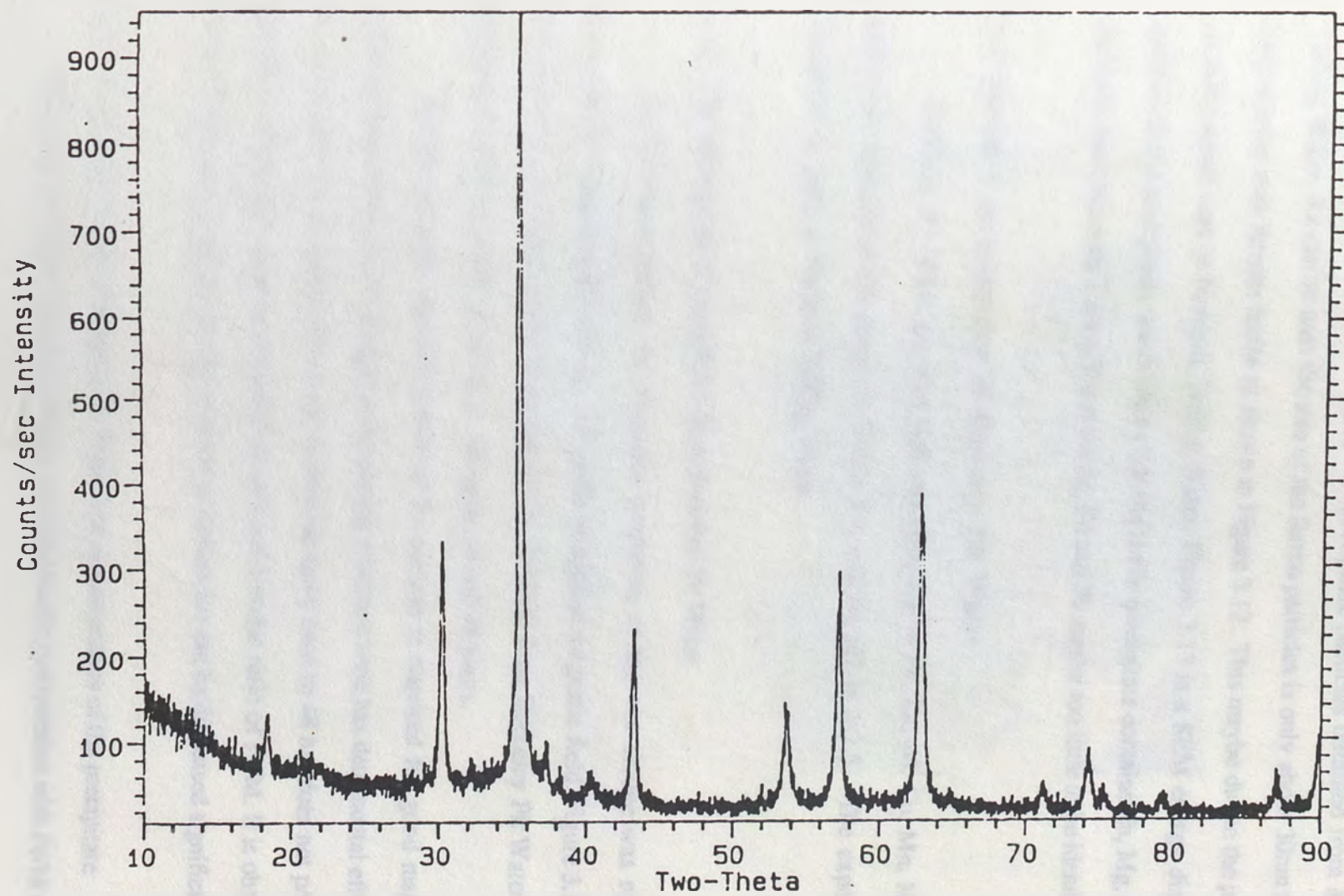


Figure 3.15. X-ray powder diffraction of precipitate obtained from ferrite coprecipitation of Noranda Tailing Water, Cu-K α

Fe^{+2} or Fe^{+3} is displaced by other metal ions in Noranda Tailing Water.

Figure 3.16. is TEM micrograph of precipitate particles obtained from Noranda Tailing Water. As can be seen the size of the ferrite particles is only about 30nm that is a little smaller than ferrous ferrite as shown in Figure 3.12.. This maybe due to the presence of other metal ions in Noranda Tailing Water. Figure 3.17 is a SEM energy dispersive analysis of the precipitate, which shows that the ferrite precipitate contains Zn, Mg, Mn, Ca elements from Noranda Tailing Water but Al, Cd and Pb maybe too little to be identified.

3.3. Ferrite Coprecipitation of Berkeley Pit Water

Berkeley Pit Water contains high concentration of Fe, Zn, Al, Cu, Mn, Mg, Ca, and small amount of Cd shown in Table 3.4. and its pH is 2-2.5. The experiment conditions is same as Noranda Tailing Water.

3.3.1. The settling rate of precipitates from Berkeley Pit Water

As discussed before, the magnetic properties of the wet sludge was roughly estimated by measuring the settling rate under an applied magnetic field. Figure 3.18 and 3.19 show that the settling rate of the precipitate obtained from Berkeley Pit Water with addition of different Fe/M molar ratios for aging 24 and 48 hours.

As can be seen, oxidation time of 20 minutes is required for good magnetic property followed by 24 hr aging time. Increasing oxidation time has detrimental effect on magnetic property of sludge. However, increasing aging time to 48 hrs does not produce significant difference between the addition of 3 and 5 molar ratio of Fe/M. It is observed that by giving longer aging time, the addition of ferrous ion can be decreased significantly.

3.3.2. The results of treated Berkeley Pit Water and characteristics of the precipitate

Berkeley Pit Water was treated by the modified ferrite precipitation with Fe/M molar

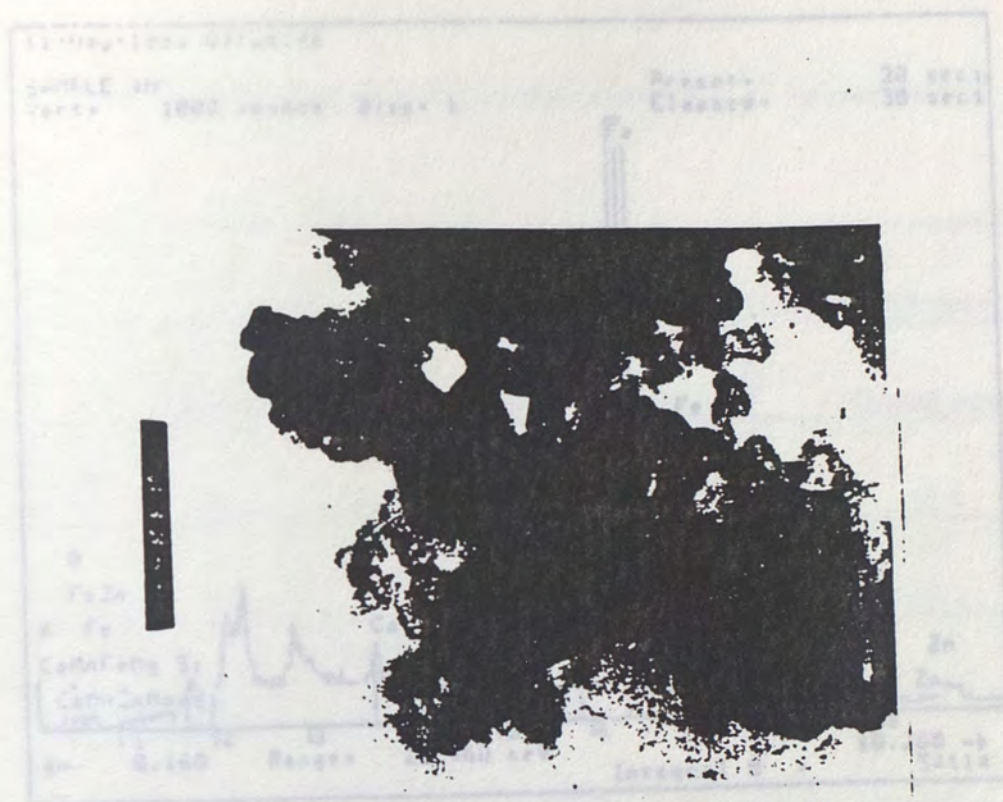


Figure 3.16. TEM micrograph (X 145k) of precipitate obtained from ferrite coprecipitation of Noranda Tailing Water

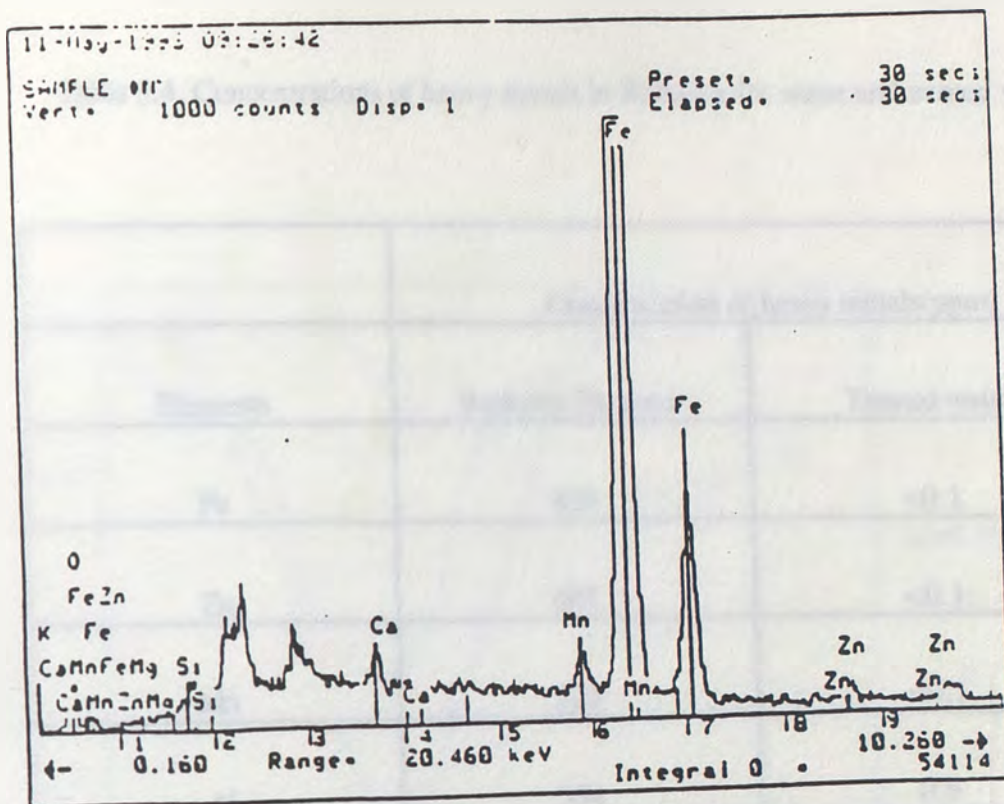


Figure 3.17. SEM energy dispersive analysis of precipitate obtained from ferrite coprecipitation of Noranda Tailing Water

Table 3.4. Concentrations of heavy metals in Berkeley Pit water and treated water

| Elements | Concentration of heavy metals(ppm) | |
|----------|------------------------------------|---------------|
| | Berkeley Pit water | Treated water |
| Fe | 439 | <0.1 |
| Zn | 607 | <0.1 |
| Mn | 223 | <0.1 |
| Al | 334 | 0.9 |
| Cd | 3.1 | <0.1 |
| Cu | 186 | <0.1 |
| Mg | 497 | 13.7 |
| Ca | 270 | 126 |

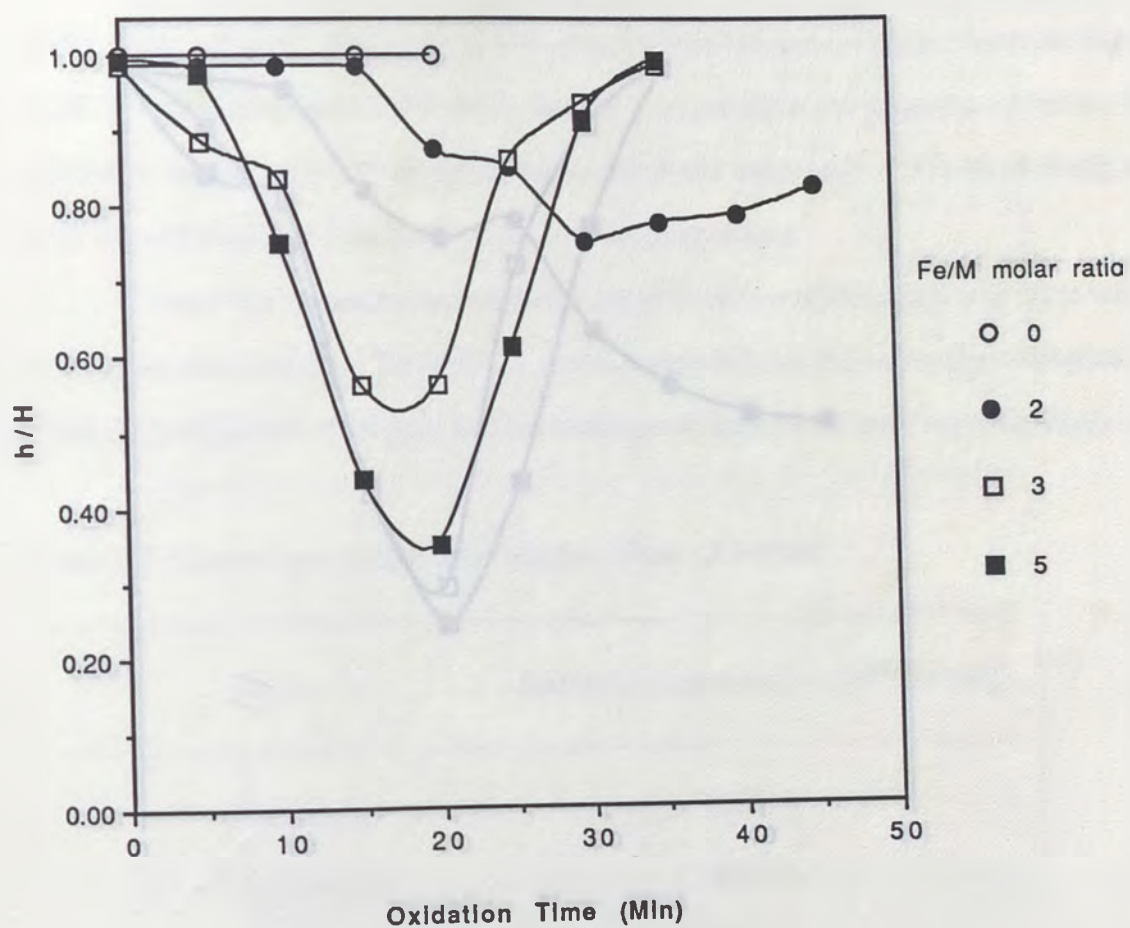


Figure 3.18. Effect of oxidation time on settling height ratio of precipitates after 24hr aging obtained from Berkeley Pit water

ratio of 5, and the resulting concentrations of heavy metals of Berkeley Pit Water and treated water are given in Table 3.4. The metal ions were completely removed by modified ferrite precipitation except for Mg and Ca ions which are not concerned by various industrial standards at the present time.

The magnetic properties of ferrite precipitates obtained with different addition of Fe/M molar ratio was measured by vibrating sample magnetometer as shown in Figure 3.20. The precipitates with Fe/M molar ratio of 0, 2, 3 and 5 do not show the magnetic of ferrite. The saturation magnetization of ferrite precipitates with Fe/M molar ratio of 3 is 36.15 emu/g and with the molar ratio of 5 is 28.5 emu/g at room temperature.

Comparing the saturation magnetization of ferrite precipitates from acid mine waters with the pure ferrite in Table 3.2, it can be concluded that the saturation magnetization of ferrite precipitates is very good and the ferrite precipitates have many applications.

Table 3.5. Comparison of Saturation Magnetization of Ferrites

Ferrite Saturation Magnetization (20°C, emu/g)

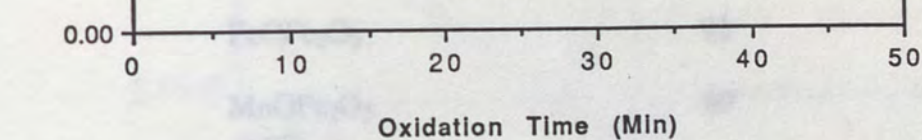


Figure 3.19. Effect of oxidation time on settling height ratio of precipitates after 48hr aging obtained from Berkeley Pit water

Ferrite Precipitates
from Acid Mine Water

ratio of 5, and the resulting concentrations of heavy metals of Berkeley Pit Water and treated water are given in Table 3.4. The metal ions were completely removed by modified ferrite precipitation except for Mg and Ca ions which are not concerned by various industrial standards at the present time.

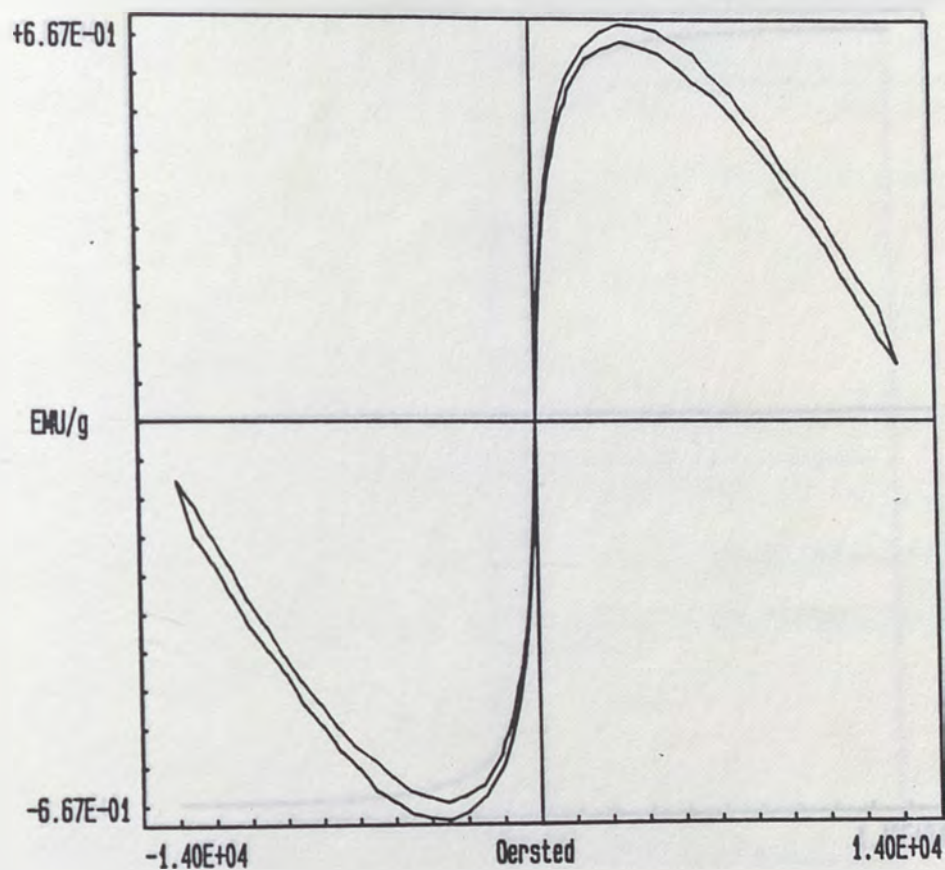
The magnetic properties of ferrite precipitate obtained with different addition of Fe/M molar ratio was measured by Vibrating Sample Magnetometer as shown in Figure 3.20. The precipitate with Fe/M molar ratio of 2 do not show the magnetic of ferrite. The saturation magnetization of ferrite precipitate with Fe/M molar ratio of 3 is 36.15 emu/g and with the molar ratio of 5 is 29.49 emu/g at room temperature.

Comparing the saturation magnetization of ferrite precipitate from acid mine waters with some pure ferrites in Table 3.5., it can be concluded that the saturation magnetization of ferrite precipitate is very good and the ferrite precipitate should have many applications.

Table 3.5. Comparison of Saturation Magnetization of Ferrites

| Ferrite | Saturation Magnetization (20°C, emu/g) |
|---|--|
| FeOFe_2O_3 | 92 |
| MnOFe_2O_3 | 80 |
| CuOFe_2O_3 | 25 |
| MgOFe_2O_3 | 27 |
| ZnOFe_2O_3 | 0 |
| Ferrite Precipitate from Acid Mine Water | 30-60 |

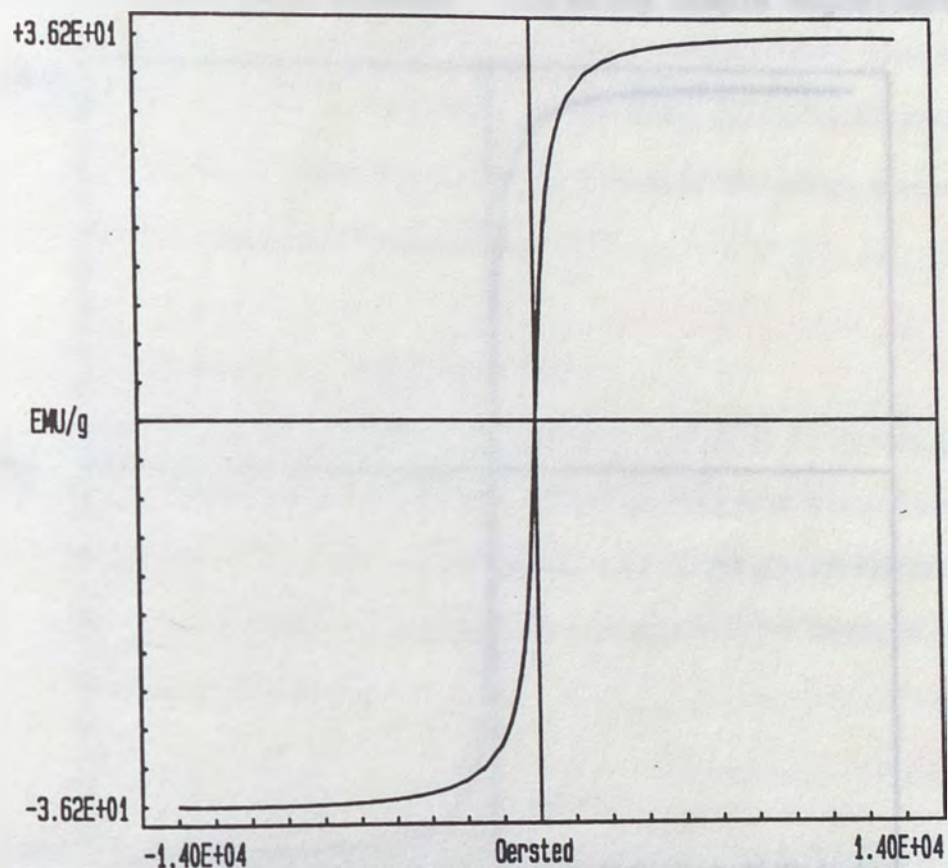
Digital Measurement Systems Vibrating Sample Magnetometer



(a) Fe/M molar ratio: 2

Figure 3.20. Magnetization curve of precipitate obtained from ferrite coprecipitation of Berkeley Pit Water

Digital Measurement Systems Vibrating Sample Magnetometer



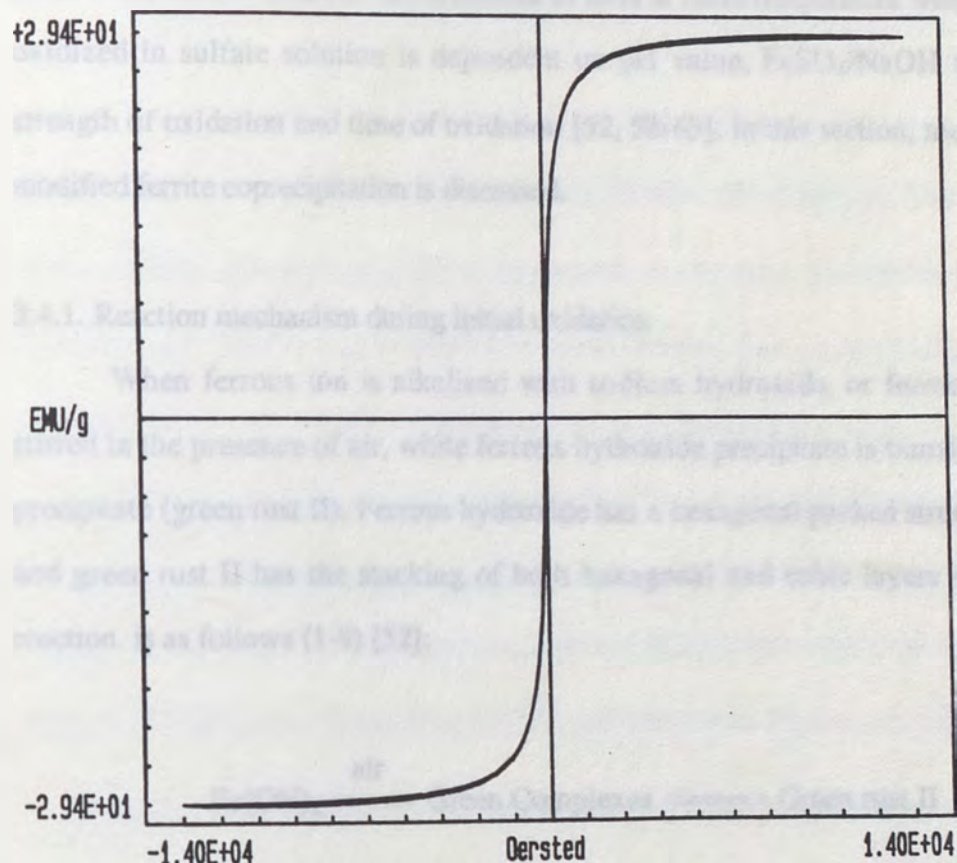
(b) Fe/M molar ratio: 3

Figure 3.20. Magnetization curve of precipitate obtained from
ferrite coprecipitation of Berkeley Pit Water

3.4. Mechanism of New Modified Ferrite Coprecipitation

In section 1.3.3, some mechanisms of ferrite precipitation have been introduced. In this section, the formation mechanism of various iron oxides and hydroxides of iron

Digital Measurement Systems Vibrating Sample Magnetometer



(c) Fe/M molar ratio: 5

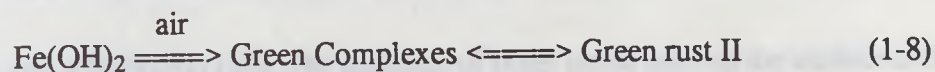
Figure 3.20. Magnetization curve of precipitate obtained from ferrite coprecipitation of Berkeley Pit Water

3.4. Mechanism of New Modified ferrite Coprecipitation

In section 1.5.2, some mechanism of ferrite precipitation have been introduced. In fact, the formation mechanism of various iron oxides and oxyhydroxides at room temperature has been an important subject in the field of corrosion of iron and steel for long time. What kind of oxide or oxyhydroxide to form at room temperature when ferrous ion is oxidized in sulfate solution is dependent on pH value, $\text{FeSO}_4/\text{NaOH}$ initial ratio, or strength of oxidation and time of oxidation [52, 58-63]. In this section, mechanism of the modified ferrite coprecipitation is discussed.

3.4.1. Reaction mechanism during initial oxidation

When ferrous ion is alkalized with sodium hydroxide, or ferrous hydroxide is stirred in the presence of air, white ferrous hydroxide precipitate is transformed to green precipitate (green rust II). Ferrous hydroxide has a hexagonal packed structure of oxygen and green rust II has the stacking of both hexagonal and cubic layers of oxygen. The reaction is as follows (1-8) [52]:



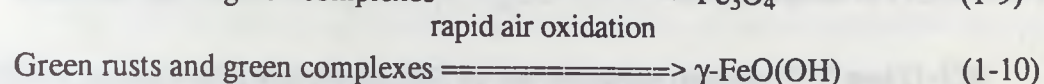
Green rust II contains both ferrous and ferric ions and sulfate ion [59]. Tamaura et al [50] gave the general formula of green rust II as $(\text{Fe}^{3+})_1(\text{Fe}^{2+})_2(\text{SO}_4^{2-})(\text{OH}^-)_{5-2n}(\text{O}^{2-})_n$, but Olowe [59,63] thought that green rust II have different formula at different conditions.

If there are other metal ions present in the solution, they will be adsorbed on the surface of green rust II [64,65] and react with ferrous ion to form mixed green rust II [38].

3.4.2. Reaction mechanism during air oxidation

After formation of green rust II, both green rust II and green complexes can be converted into Fe_3O_4 by slow air oxidation and into $\gamma\text{-FeO(OH)}$ by rapid air oxidation [52].

The reactions are expressed in (1-9) and (1-10):



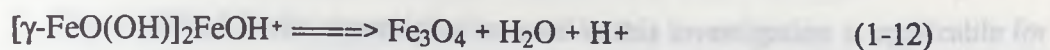
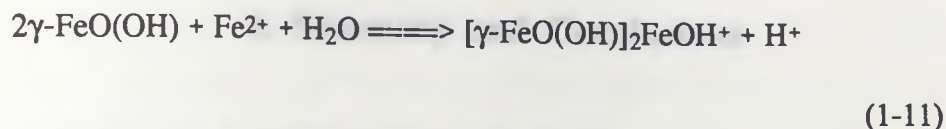
The green rust II has hexagonal structure containing cubic layer of oxygen. The Fe_3O_4 has inverse spinel structure with f.c.c framework of oxygen. The $\gamma\text{-FeO(OH)}$ has orthorhombic structure with f.c.c. framework of oxygen. Therefore, green rust II is transformed Fe_3O_4 and $\gamma\text{-FeO(OH)}$ more readily than to $\alpha\text{-FeOOH}$, which has orthorhombic structure based on hexagonal closed packed oxygen layer.

Prolonged oxidation will convert Fe_3O_4 and $\gamma\text{-FeO(OH)}$ to $\alpha\text{-FeO(OH)}$ or $\delta\text{-FeO(OH)}$, and decrease magnetic property.

If other metal ions are present, some of them other metals ion will adsorb on the surface of Fe_3O_4 and $\gamma\text{-FeO(OH)}$ [64,65] and react with Fe_3O_4 and $\gamma\text{-FeO(OH)}$ to form mixed Fe_3O_4 and $\gamma\text{-FeO(OH)}$ [38]. The presence of other metal ions on the surface and in the lattice of Fe_3O_4 and $\gamma\text{-FeO(OH)}$ prolongs oxidation time.

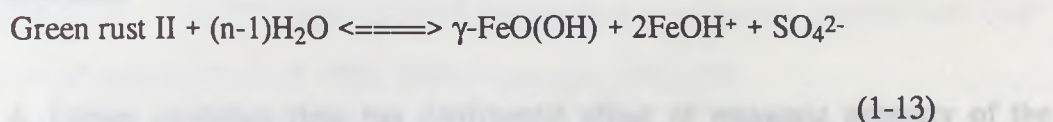
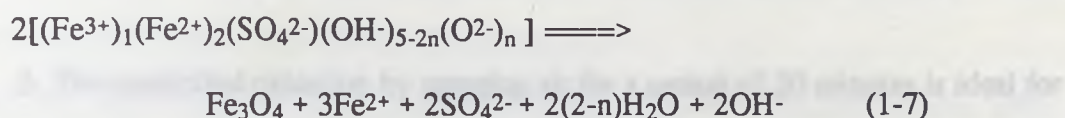
3.4.3. Reaction mechanism during aging

During aging, the adsorbed $\text{Fe}^{\text{II}}\text{-}\gamma\text{-FeO(OH)}$ or $\text{M}^{\text{II}}\text{-}\gamma\text{-FeO(OH)}$ or mixed $\gamma\text{-FeO(OH)}$ is subsequently transformed to Fe_3O_4 or mixed ferrite. The reactions of the transformation are expressed in (1-11) and (1-12):

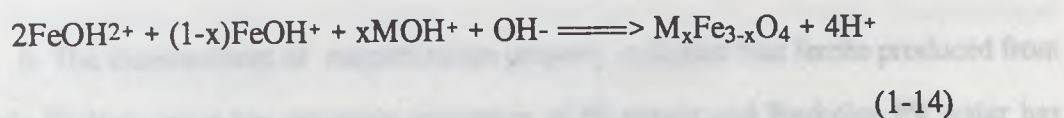


These reactions can be substantiated by the slow decrease of pH value in aging.

If residual green rust II is present, the green rust II will decompose to Fe_3O_4 and $\gamma\text{-FeO(OH)}$ or mixed Fe_3O_4 and $\gamma\text{-FeO(OH)}$ by the following reaction (1-7) and (1-13):



The decomposed Fe^{2+} and other M^{2+} ions are hydrolyzed to FeOH^+ and MOH^+ , then some FeOH^+ and MOH^+ ions are adsorbed on the surface of Fe_3O_4 and $\gamma\text{-FeO(OH)}$. Some of the adsorbed FeOH^+ ions are oxidized to FeOH^{2+} ions by the dissolved oxygen. These hydrolyzed ions finally form stable Fe_3O_4 or mixed ferrite following reaction (1-14):



Because there are other metal ions on the surface and in the lattice of Fe_3O_4 and $\gamma\text{-FeO(OH)}$, the corresponding aging time is much longer than that when there were be no other metal ions.

4. Summary and Conclusions

1. The modified ferrite coprecipitation used in this investigation is applicable for treatment of acid mine waters and other industrial effluents containing heavy metals.
2. The coprecipitation and transformation to ferrite can be accomplished at room temperature and at a relatively short time.
3. The controlled oxidation by sparging air for a period of 20 minutes is ideal for ferrite formation.
4. Larger oxidation time has detrimental effect of magnetic property of the precipitate.
5. At an appropriate conditions the heavy metals present in the Noranda Tailing and Berkeley Pit waters can be converted to valuable ferrite.
6. The measurement of magnetization property indicated that ferrite produced from Noranda Tailing water has magnetic saturation of 60 emu/g and Berkeley Pit water has magnetic saturation of 36 emu/g.

References

1. Kleinman, R. L. P., " Acid Mine Drainage", E&MJ, July 1989, 16j-16N.
2. Chalkey, M. E. et al., "Tailings and Effluent Management", Proceedings of the International Symposium, Vol.4, Halifax, CIM, August 20-24, 1989, Pergamon Press
3. Gadsby, J. W. et al., " Acid Mine Drainage: Designing for Closure", BiTech Publishers, 1990.
4. Onysko, S. J., "Chemical abatement of Acid Mine Drainage Formation", PhD Dissertation 1985., Univ. of California, Berkeley.
5. Kelly, M., "Mining and the Fresh water Environment". Elsevier Applied Science, 1988.
6. Skousen, J. G., " An Evaluation of Acid mine Drainage treatment Systems and Cost" Environmental management of 1990, SME, Colorado, 1991, p173.
7. Cushnie, G. C., "Removal of Metals from waste water: Neutralization and Precipitation", Pollution Tech. Review, Noys Publication, 1989.
8. Okuda, T., Sugano, I. and Tsuji, T., "Removal of Heavy Metals from Wastewater by Ferrite Coprecipitation" Filtration and Separation, p472, Sept/Oct. 1975.
9. Tsuji, T., "Ferrite-Technology Applications and Their Expansion from Electronic to Civil Engineering Fields", Advances in Ceramics, Vol.15,, Fourth International Conference on Ferrite, part I, Edited by F. Y. Wang, p573-581.
10. Cullity, B. D., "Introduction to Magnetic Materials", Addison-Wesley publishing Company, 1972.
11. Jakubovics, J. P., "Magnetism and Magnetic Materials", The Institute of Metals, 1987.
12. Goldman, A., "Modern ferrite Technology", Van Nostrand Reinhold, 1990.
13. Kondo, Y. et al., " Magnetic Marker Systems Using By-Product Ferrite", Advances in Ceramics, Vol.15, Fourth International Conference on Ferrite, part I, Edited by F. Y. Wang, p589-594.

14. Yamauchi, F. and Nakano, S., "Magnetic Marker Using Ferrite Byproduct and its application", Proceedings of the International Conference in Ferrites, Tokyo, Japan, 1980, p894-97.
15. Yamauchi, F. and Yokoyama, K., "Ferrite-Resin Composite Material for Vibration Damping and its Applications", Bull. Jpn. Soc. Precis. Eng. V17 n3 Sep. 1983 p147-153.
16. Hatakeyama, K. and Inui, T., "Electromagnetic Wave Absorber using Ferrite Absorbing Material Dispersed with short Metal Fibers", IEEE Transactions on Magnetic, Vol. Mag-20, No.5. September 1984, p1261-1263.
17. Jha, V. and Banthia, A. K., "Composites Based on Waste-Ferrites as Microwave Absorber", Advances in Ferrite, International Conference on Ferrite, 1989, India, p961-965.
18. Tsutaoka, T. Ema, S. and Sato, H., "Physical and Chemical Properties of Magnetic Fluid and Possibility for some Applications", Advances in Ferrite, International Conference on Ferrite, 1989, India, p1113-1118.
19. Takada, T. and Kiyama, M., "Preparation of Ferrites by the Wet Method", Proceeding of The international Conference on Ferrites, 1970, p69-71.
20. Akashi, T. et al, "Low-Loss and high-Stability Manganese-Zinc Ferrites", Proceeding of The international Conference on Ferrites, 1970, p183-6.
21. Sato, T. Kuroda, C. and Saito, M., "Preparation and Magnetic Characteristics of Ultra-Fine Spinel Ferrites", Proceeding of The international Conference on Ferrites, 1970, p72-74.
22. Kiyama, M., "The Formation of Manganese and Cobalt Ferrites by the Air Oxidation of Aqueous Suspensions and Their Properties", Bull. Chem. Soc. Jpn., 51, p134-138 (1978).
23. Kaneko, K. and Katsura, T., "The Formation of Mg-bearing Ferrite by the Air Oxidation of Aqueous Suspensions", Bull. Chem. Soc. Jpn., 52, p747-752 (1979).

24. Kaneko, K. et al., "The Formation of Cd-bearing Ferrite by the Air Oxidation of an Aqueous Suspensions", Bull. Chem. Soc. Jpn., 52, p1080-1085 (1979).
25. Tamaura, Y. and Katsura, T., "Formation of Lead-bearing Ferrite in Aqueous Suspension by Air Oxidation", J. Chem. Soc. Dalton Trans., p825-828(1980).
26. Kanzaki, T. et al., "Formation of Zn-bearing Ferrite by Air Oxidation of Aqueous Suspension", Bull. Chem. Soc. Jpn., 54, p135-137 (1981).
27. Kanzaki, T., Furukawa, H. and Katsura, T., "Formation of Molybdenum-bearing Ferrite, $\text{Fe}_{3-x}\text{Mo}_x\text{O}_4$ (0.04-0.19), in Aqueous Suspension by Air Oxidation", J. Chem. Soc. Dalton Trans., p1197-1198 (1983).
28. Pandya, P. B., Joshi, H. H. and Kulkarni, R. G., "Magnetic and Structural Properties of CuFe_2O_4 Prepared by the Co-Precipitation Method", J. Mater. Sci. Let. 10(1991) p474-476.
29. Katsura, T. Tamaura, Y. and Chyo, G. S., "The Formation of the Oxidized Fe_3O_4 - Fe_2TiO_4 Solid Solution by the Air Oxidation Of the Aqueous Suspension", Bull. Chem. Soc. Jpn., 52, p96-100 (1979).
30. Tamaura, Y. Rasyid, U. and Katsura, T., "Formation of a Chromium-bearing Ferrite, $\text{Cr}_{0.42}\text{Fe}_{2.56}\text{O}_{4.00}$, in Aqueous Suspension by Nitrate Oxidation", J. Chem. Soc. Dalton Trans., p2125-2128 (1980).
31. Ito, K. et al., "Formation of Aluminum-bearing Ferrite in Aqueous Suspension by Air oxidation", J. Chem. Soc. Dalton Trans., p2217-2219 (1980).
32. Tamaura, Y., Mechaimonchit, S. and Katsura, T., "The Formation of V-bearing Ferrite by Aerial Oxidation of an Aqueous Suspension", J. Inorg. Nucl. Chem., 43, p671-675 (1981).
33. Robbins, H., "The Preparation of Mn-Zn Ferrites by Co-Precipitation", Ferrites: Proceedings of the International Conference, Sept-Oct. 1980, Japan, p7-10.

34. Ito, K., Tamaura, Y. and Katsura, T., "Formation of Zinc(II)-Bearing Ferrites From γ -FeO(OH)", J. Chem. Soc. Dalton Trans., p987-989 (1983).
35. Ito, K., Tamaura, Y. and Katsura, T., "Cadmium(II)-, Magnesium-, and Zinc(II)-bearing Ferrites Formed from γ -FeOOH at Various Reaction pH's", Bull. Chem. Soc. Jpn., 57, p2820-2824 (1984).
36. Tamaura, Y., "Zn^{II}-bearing Green Rust II and Its Spontaneous Transformation into Zn^{II}-bearing Ferrite in Aqueous Solution", Bull. Chem. Soc. Jpn., 58, p2951-2954 (1985).
37. Tamaura, Y., "Ni(II)-Bearing Green Rust II and Its Spontaneous Transformation into Ni(II)-Bearing Ferrites", Bull. Chem. Soc. Jpn., 59, p1829-1832 (1986).
38. Tamaura, Y., "New Ferrite-Formation Reactions In the Suspensions of γ -FeOOH and 'Green Rust II'", Advances in Ceramics, Vol.15, Fourth International Conference on Ferrite, part I, Edited by F. Y. Wang, p87-92.
39. Tamaura Y., "Ferrite Formation from the Intermediate, Green II, in the Transformation Reaction of γ -FeO(OH) in Aqueous Suspension", Inorg. Chem., 1985, 24, p4363-4366.
40. Takada, T., "Development and Application of Synthesizing Technique of Spinel Ferrites by the Wet Method", Proceedings of the International Conference, Sept-Oct. 1980, Japan, p3-6.
41. Tamaura, Y. and Abe, H., "Solidification of Heavy Metal Ions into Stabilized Ferrite Sludge", Advances in Ferrite, International Conference on Ferrite, 1989, India, p1173-1178.
42. Tamaura, Y. et al., "Ferrite Process; Heavy Metal Ions Treatment System", Wat. Sci. Tech., Vol.23, 1991, p1893-1900.
43. Mehta, R. K. et al., "Removal of Heavy Metal Ions from Oil Shale Process",

Proceedings 1991 Eastern Oil Shale Symposium, Nov, 13-15, p362-366.

44. Mehta, R. K., Zhang, L. and Warren, G. W., " Chemoremediation of Acid Mine Drainage by Controlled Ferrite Coprecipitation and Magnetic Separation", SAE Annual Meeting, Phoenix, Arizona, Feb. 24-27, 1992.
45. Ito, S., Kikuchi, A. and Yoneda, N., "Continuous Treatment on Magnetic Separation of Heavy Metal Ions in water", AIChE Symposium Series, No.243, Vol. 81. p133-138.
46. Sano, M., "Recovering Ferrite Material from Mine Drainage", Advances in Ceramics, Vol.15, Fourth International Conference on Ferrite, Part I, Edited by F.Y.Wang, 583-588.
47. Kiyama, M., "Conditions for the Formation of Fe_3O_4 by the Air Oxidation of $\text{Fe}(\text{OH})_2$ Suspensions", Bull. Chem. Soc. Jpn., 47(7), p1646-1650 (1974).
48. Tamaura, Y., Chyo, G. S. and Katsura, T., "The Fe_3O_4 -Formation by the 'Ferrite Process': Oxidation of the Reactive $\text{Fe}(\text{OH})_2$ Suspension Induced by Sucrose", Water Research, Vol.13, p21-31 (1979).
49. Tamaura, Y., Buduan, P. V. and Katsure, T., "Studies on the Oxidation of Iron(II) Ion during the Formation of Fe_3O_4 and $\alpha\text{-FeO}(\text{OH})$ by Air Oxidation of $\text{Fe}(\text{OH})_2$ Suspensions", J. Chem. Soc. Dalton Trans., p1807-1811 (1981).
50. Tamaura, Y. Yoshida, T. and Katsura, T., "The Synthesis of Green Rust II($\text{Fe}^{\text{III}}_1\text{-Fe}^{\text{II}}_2$) and Its Spontaneous Transformation into Fe_3O_4 ", Bull. Chem. Soc. Jpn., 57(9), p2411-2416 (1984).
51. Bernal, J. D., Dasgupta, D. R. and Mackay, A. L., "The Oxides and Hydroxides of Iron and Their Structural Inter-Relationships", Clay Miner. Bull. 4, 15 (1959).
52. Misawa, T., Hashimoto, K. and Shimodaira, S., " The Mechanism of Formation of Iron Oxide and Oxyhydroxides in Aqueous Solutions at Room Temperature" Corrosion Science, 1974, Vol.14, 131-149.
53. Tamaura, Y., Ito, K. and Katsura, T., "Transformation of $\gamma\text{-FeO}(\text{OH})$ to Fe_3O_4 by

Adsorption of Iron(II) Ion on γ -FeO(OH)", J. Chem. Soc. Dalton Trans., p189-194 (1983).

54. Tamaura, Y. et al., "The Transformation of γ -FeO(OH) to Fe₃O₄ and Green Rust II in an Aqueous Solution", Bull. Chem. Soc. Jpn., 57(9), p2417-2421 (1984).

55. Abe, M. and Tamaura, Y., "Ferrite Plating in aqueous solution: New Technique for preparing Magnetic Thin Film", J. Appl. Phys., 55(1984), p2614-2616.

56. Tamaura, Y., Itoh, T. and Abe, M., "Reaction Mechanism of Ferrite-Formation by Oxidation of Fe(II) Ion in Aqueous Solution", Advances in Ferrite, International Conference on Ferrite, 1989, India, p83-88.

57. Instructions of Fisher Accumet pH Meter, Fisher Scientific.

58. Misawa, T., "The Thermodynamic Consideration For Fe-H₂O System At 25°C", Corrosion Science, 13(1973), p695-676.

59. Olowe, A. A. and Genin, J. M. R., " The Mechanism of Oxidation of Ferrous Hydroxide in Sulphated Aqueous Media: Importance of the Initial Ratio of the Reactions", Corrosion Science, 32(1991), No. 9, p965-984.

60. Olowe, A. A., Pauron, B. and Genin, J. M. R., " The Influence of Temperature on the Oxidation of Ferrous Hydroxide in Sulphated aqueous Medium: Activation Energies of Formation of the Products and Hyperfine Structure of Magnetite", Corrosion Science, 32(1991), No. 9, p985-1001.

61. Olowe, A. A., Refait, Ph. and Genin, J. M. R., " The Influence of Concentration on the Oxidation of Ferrous Hydroxide in Basic Sulphated Medium: Particle Size Analysis of Goethite and δ -FeOOH", Corrosion Science, 32(1991), No. 9, p1003-1020.

62. Olowe, A. A. and Genin, J. M. R., "The Influence of Concentration on the Oxidation of Ferrous Hydroxide in Acidic Sulphated Medium: Particle Size Analysis of Lepidocrocite", Corrosion Science, 32(1991), No. 9, p1021-1028.

63. Olowe, A. A. and Genin, J. M. R., "Potential-pH Equilibrium Diagrams for the Iron-Water System in the Presence of Sulfate Ions: Domain of Existence of Green Rust 2", Int'l Sym CORROSION SCIENCE AND ENGINEERING, Brussels, Mar.12-15, 1989. Edited by R. A. Rapp, N. A. Gokcen and A. Pourbaix, Published by CEBELCOR, Avenue Paul Heger, Grille 2, 1050 Bruxelles, Belgique. Vol. 1, p. 363-380.
64. Davis, J. A. and Leckie, J. O., "Surface Ionization and Complexation at the Oxide/Water Interface, II. Surface Properties of Amorphous Iron Oxyhydroxide and Adsorption of Metal Ions", J. of Colloid and Interface Science, Vol. 67, No.1, Oct. 15, 1978, p91-107.
65. Benjamin, M. M. and Leckie, J. O., "Multiple-Site Adsorption of Cd, Cu, Zn, and Pb on Amorphous Iron Oxyhydroxide", J. of Colloid and Interface Science, Vol. 79, No.1, Jan. 15, 1981, p209-221.